The *Drosophila* SWI/SNF chromatin-remodeling complexes BAP and PBAP play separate roles in regulating growth and cell fate during regeneration

Running Title: SWI/SNF regulates regeneration

Yuan Tian[1] and Rachel K. Smith-Bolton[1,2*]

[1]Department of Cell and Developmental Biology, University of Illinois at Urbana-Champaign, Urbana, IL, USA

[2]Carl R. Woese Institute for Genomic Biology

*Author for correspondence: rsbolton@illinois.edu

Key words

regeneration, chromatin, SWI/SNF complexes, cell fate, *Drosophila*, wing imaginal disc

Summary statement

During regeneration of the *Drosophila* wing disc, the SWI/SNF PBAP complex is required for regenerative growth and expression of JNK signaling targets, while the BAP complex maintains posterior cell fate.

Abstract

To regenerate, damaged tissue must heal the wound, regrow to the proper size, replace the correct cell types, and return to the normal gene-expression program. However, the mechanisms that temporally and spatially control the activation or repression of important genes during regeneration are not fully understood. To determine the role that chromatin modifiers play in regulating gene expression after tissue damage, we induced ablation in *Drosophila* imaginal wing discs, and screened for chromatin regulators that are required for epithelial tissue regeneration. Here we show that many of these genes are indeed important for promoting or constraining regeneration. Specifically, the two SWI/SNF chromatin-remodeling complexes play distinct roles in regulating different aspects of regeneration. The PBAP complex regulates regenerative growth and developmental timing, and is required for the expression of JNK signaling targets and the growth promoter *Myc*. By contrast, the BAP complex ensures correct patterning and cell fate by stabilizing expression of the posterior gene *engrailed*. Thus, both SWI/SNF complexes are essential for proper gene expression during tissue regeneration, but they play distinct roles in regulating growth and cell fate.

Introduction

Regeneration is a complex yet highly elegant process that some organisms can use to recognize, repair and replace missing or damaged tissue. Imaginal disc repair in *Drosophila* is a good model system for understanding regeneration due to the high capacity of these tissues to regrow and restore complex patterning, as well as the genetic tools available in this model organism (Hariharan and Serras, 2017). Regeneration requires the coordinated expression of genes that regulate the sensing of tissue damage, induction of regenerative growth, repatterning of the tissue, and coordination of regeneration with developmental timing. Initiation of regeneration in imaginal discs requires known signaling pathways such as the ROS, JNK, Wg, p38, Jak/STAT, and Hippo pathways (Bergantinos et al., 2010; Bosch et al., 2008; Grusche et al., 2011; Katsuyama et al., 2015; Santabárbara-Ruiz et al., 2015; Schubiger et al., 2010; Smith-Bolton et al., 2009; Sun and Irvine, 2011). These pathways activate many regeneration genes, such as the growth promoter Myc (Smith-Bolton et al., 2009) and the hormone-like peptide *ilp8*, which delays pupariation after imaginal disc damage (Colombani et al., 2012; Garelli et al., 2012). However, misregulation of these signals can impair regeneration. For example, elevated levels of JNK signaling can induce patterning defects in the posterior of the wing (Schuster and Smith-Bolton, 2015), and elevated ROS levels can suppress JNK activity and regenerative growth (Brock et al., 2017). While the signals that initiate regeneration have been extensively studied, regulation of regeneration gene expression in response to tissue damage is not fully understood.

Such regulation could occur through chromatin modification. In *Drosophila*, chromatin modifiers include the repressive complexes PRC1 and PRC2, the

activating complexes TAC1, COMPASS and COMPASS-like, and the SWI/SNF chromatin remodelers BAP and PBAP (Kassis et al., 2017). PRC2 carries out trimethylation of histone H3 at lysine 27, recruiting PRC1 to repress transcription of nearby genes. COMPASS-like and COMPASS carry out histone H3 lysine 4 monomethylation and di- and trimethylation, respectively, thereby activating expression of nearby genes. TAC1 acetylates histone H3 lysine 27, also supporting activation of gene transcription. BAP and PBAP alter or move nucleosomes to facilitate binding of transcription factors and chromatin modifiers. Rapid changes in gene expression induced by these complexes may help facilitate a damaged tissue's regenerative response.

A few chromatin modifiers and histone modifications have been reported to be important for regulating regeneration of Xenopus tadpole tails, mouse pancreas and liver, zebrafish fins, and *Drosophila* imaginal discs (Blanco et al., 2010; Fukuda et al., 2012; Jin et al., 2015; Pfefferli et al., 2014; Scimone et al., 2010; Skinner et al., 2015; Stewart et al., 2009; Tseng et al., 2011; Wang et al., 2008). Furthermore, components of *Drosophila* and mouse SWI/SNF complexes regulate regeneration in the *Drosophila* midgut and mouse skin, liver, and ear (Jin et al., 2013; Sun et al., 2016; Xiong et al., 2013). However, little is known about how these complexes alter gene expression, signaling, and cellular behavior to regulate regeneration. Importantly, genome-wide analysis of chromatin state after *Drosophila* imaginal disc damage revealed changes in chromatin around a large set of genes, including known regeneration genes (Vizcaya-Molina et al., 2018). Thus, chromatin modifiers likely play a key role in regulating activation of the regeneration program. However, it is unclear whether all regeneration genes are coordinately regulated in the same manner, or whether specific chromatin

105 modification complexes target different subsets of genes that respond to tissue
106 damage.
107
108 To probe the role of chromatin modifiers in tissue regeneration systematically, we
109 assembled a collection of pre-existing *Drosophila* mutants and RNAi lines target-
110 ing components of these complexes as well as other genes that regulate chroma-
111 tin, and screened these lines for regeneration defects using the *Drosophila* wing
112 imaginal disc. We used a spatially and temporally controllable tissue-ablation
113 method that uses transgenic tools to induce tissue damage only in the wing pri-
114 mordium (Smith-Bolton et al., 2009). This method ablates 94% of the wing pri-
115 mordium on average at the early third instar and allows the damaged wing discs
116 to regenerate *in situ*. Previous genetic screens using this tissue ablation method
117 have identified genes critical for regulating different aspects of regeneration, such
118 as *taranis*, *trithorax*, and *cap-n-collar*, demonstrating its efficacy in finding regen-
119 eration genes (Brock et al., 2017; Schuster and Smith-Bolton, 2015; Skinner et
120 al., 2015).
121
122 Through this targeted genetic screen of chromatin regulators we found that muta-
123 tions in *Drosophila* SWI/SNF components caused striking regeneration defects.
124 The SWI/SNF complexes are conserved multi-subunit protein complexes that ac-
125 tivate or repress gene expression (Wilson and Roberts, 2011) by using the en-
126 ergy from ATP hydrolysis to disrupt histone-DNA contacts and remodel nucleo-
127 some structure and position (Côté et al., 1994; Kwon et al., 1994). Brm is the
128 only ATPase of the SWI/SNF complexes in *Drosophila* (Kassis et al., 2017;
129 Tamkun et al., 1992). Moira (Mor) serves as the core scaffold of the complexes
130 (Mashtalir et al., 2018). Other components contain domains involved in protein-

protein interactions, protein-DNA interactions, or interactions with modified histones (Hargreaves and Crabtree, 2011). There are two subtypes of SWI/SNF in *Drosophila*: the Brahma-associated proteins (BAP) and the Polybromo-associated BAP (PBAP) remodeling complexes (Collins and Treisman, 2000; Mohrmann et al., 2004). They share common core components, including Brm, Snr1, Mor, Bap55, Bap60, Bap111 and Actin (Mohrmann et al., 2004), but contain different signature proteins. The PBAP complex is defined by the components Bap170, Polybromo and Sayp (Mohrmann et al., 2004; Chalkley et al., 2008). Osa defines the BAP complex (Collins et al., 1999; Vázquez et al., 1999).

Here we show that the SWI/SNF complexes BAP and PBAP are required for regeneration, and that the two complexes play distinct roles. The PBAP complex is important for activation of JNK signaling targets such as *ilp8* to delay metamorphosis and allow enough time for the damaged tissue to regrow, and for expression of *myc* to drive regenerative growth. By contrast, the BAP complex is not required for regenerative growth, but instead functions to prevent changes in cell fate induced by tissue damage through stabilizing expression of the posterior identity gene *engrailed*. Thus, different aspects of the regeneration program are regulated independently by distinct chromatin regulators.

Materials and Methods

Fly stocks

The following fly stocks were obtained for this study. In some cases they were rebalanced before performing experiments: *w^{1118};; rnGAL4, UAS-rpr, tub-GAL80^{ts}/TM6B, tubGAL80* (Smith-Bolton et al., 2009), *w^{1118}* (Wild type), *w^{*}; P{neoFRT}82B osa^{308}/TM6B, Tb^{1}* (Bloomington *Drosophila* stock center,

BL#5949) (Treisman et al., 1997), *w*; Bap170$^{\Delta 135}$/T(2;3)SM6a-TM6B, Tb^{1}* was a gift from Jessica E. Treisman (Carrera et al., 2008), *brm^{2} e^{s} ca^{1}/TM6B, Sb^{1} Tb^{1} ca^{1}* (BL#3619) (Kennison and Tamkun, 1988), *mor^{1}/TM6B, Tb^{1}* (BL#3615) (Kennison and Tamkun, 1988), *y^{1} w^{1}; P{neoFRT}40A P{FRT(w^{hs})}G13 cn^{1} PBac{SAstopDsRed}Bap55^{LL05955} bw^{1}/CyO, bw^{1}* (BL#34495) (Schuldiner et al., 2008), *bap111* RNAi (Vienna *Drosophila* Resource Center, VDRC#104361), control RNAi background (VDRC#15293) *bap60* RNAi (VDRC#12673), *brm* RNAi (VDRC#37721), *P{PZ}tara^{03881} ry^{506}/TM3, ry^{RK} Sb^{1} Ser^{1}* (BL#11613) (Gutierrez, 2003), *UAS-tara* was a gift from Michael Cleary (Manansala et al., 2013), *TRE-Red* was a gift from Dirk Bohmann (Chatterjee and Bohmann, 2012). *mor^{2}*, *mor^{11}* and *mor^{12}* alleles were gifts from James Kennison (Kennison and Tamkun, 1988), *snr1^{E2}* and *snr1^{SR21}* alleles were gifts from Andrew Dingwall (Zraly et al., 2003).

The mutants and RNA interference lines in Table S1 used for the chromatin regulator screen were:

st^{1} in^{1} kni^{ri-1} Scr^{W} Pc^{3}/TM3, Sb^{1} Ser^{1} (BL#3399),

cn^{1} Psc^{1} bw^{1} sp^{1}/CyO (BL#4200),

y^{1} w; P{neoFRT}42D Psc^{e24}/SM6b, P{eve-lacZ8.0}SB1* (BL#24155),

w; P{neoFRT}82B Abd-B^{Mcp-1} Sce^{1}/TM6C, Sb^{1} Tb^{1}* (BL#24618),

w; P{neoFRT}82B Scm^{D1}/TM6C, Sb^{1} Tb^{1}* (BL#24158),

w; E(z)^{731} P{1xFRT.G}2A/TM6C, Sb^{1} Tb^{1}* (BL#24470),

w; Su(z)12^{2} P{FRT(w^{hs})}2A/TM6C, Sb^{1} Tb^{1}* (BL#24159),

esc^{21} b^{1} cn^{1}/In(2LR)Gla, wg^{Gla-1}; ca^{1} awd^{K} (BL#3623),

y^{1} w^{67c23}; P{wHy}Caf1-55^{DG25308} (BL#21275),

w^{1118}; P{XP}escl^{d01514} (BL#19163),

y^{1} w; phol^{81A}/TM3, Ser^{1} y^{+}* (BL#24164),

183 *red^{1} e^{1} ash2^{1}/TM6B, Tb^{1}* (BL#4584),

184 *w^{1118}; PBac{WH}Utx^{f01321}/CyO* (BL#18425),

185 *w*; ash1^{22} P{FRT(w^{hs})}2A/TM6C, Sb^{1} Tb^{1}* (BL#24161),

186 *w^{1118}; E(bx)$^{Nurf301-3}$/TM3, P{ActGFP}JMR2, Ser^{1}* (BL#9687),

187 *y^{1} w^{67c23}; P{lacW}Nurf-38^{k16102}/CyO* (BL#12206),

188 *Mi-2^{4} red^{1} e^{4}/TM6B, Sb^{1} Tb^{1} ca^{1}* (BL#26170),

189 *mor* RNAi (VDRC#6969),

190 *psq^{E39}/CyO; ry^{506}* (BL#7321),

191 *Rbf^{14} w^{1118}/FM7c* (BL#7435),

192 *w^{1118} P{EP}Dsp1^{EP355}* (BL#17270),

193 *cn^{1} grh^{lM} bw^{1}/SM6a* (BL#3270),

194 *y^{1} w^{67c23}; P{lacW}lolal^{k02512}/CyO* (BL#10515),

195 *w*; P{neoFRT}42D Pcl^{5}/CyO* (BL#24157),

196 *w*; HDAC1^{def24} P{FRT(w^{hs})}2A P{neoFRT}82B/TM6B, Tb^{1}* (BL#32239),

197 *w^{1118}; Sirt1$^{2A-7-11}$* (BL#8838),

198 *Eip74EF^{v4} vtd^{4}/TM3, st^{24} Sb^{1}* (BL#5050),

199 *sc^{1} z^{1} w^{is}; Su(z)2$^{1.b7}$/CyO* (BL#5572),

200 *P{PZ}gpp^{03342} ry^{506}/TM3, ry^{RK} Sb^{1} Ser^{1}* (BL#11585),

201 *y^{1} w^{1118}; P{lacW}mod(mdg4)^{L3101}/TM3, Ser^{1}* (BL#10312),

202 *w^{1118}; PBac{RB}su(Hw)^{e04061}/TM6B, Tb^{1}* (BL#18224),

203 *cn^{1} P{PZ}lid^{10424}/CyO; ry^{506}* (BL#12367),

204 *Asx^{XF23}/CyO* (BL#6041),

205 *y^{1} w^{1}; P{neoFRT}40A P{FRT(w^{hs})}G13 cn^{1} PBac{SAsto-*

206 *pDsRed}dom^{LL05537} bw^{1}/CyO, bw^{1}* (BL#34496),

207 *cn^{1} E(Pc)^{1} bw^{1}/SM5* (BL#3056),

208 *kis^{1} cn^{1} bw^{1} sp^{1}/SM6a* (BL#431),

209 *kto[1] ca[1]/TM6B, Tb[1]* (BL#3618),

210 *skd[2]/TM6C, cu[1] Sb[1] ca[1]* (BL#5047).

211

212 **Genetic screen**

213 Mutants or RNAi lines were crossed to *w[1118];; rnGAL4, UAS-rpr, tub-*

214 *GAL80[ts]/TM6B, tubGAL80* flies. Controls were *w[1118]* or the appropriate RNAi

215 background line. Embryos were collected at room temperature on grape plates

216 for 4 hours in the dark, then kept at 18°C. Larvae were picked at 2 days after egg

217 lay into standard Bloomington cornmeal media and kept at 18°C, 50 larvae in

218 each vial, 3 vials per genotype per replicate. On day 7, tissue ablation was in-

219 duced by a placing the vials in a 30°C circulating water bath for 24 hours. Then

220 ablation was stopped by placing the vials in ice water for 60 seconds and return-

221 ing them to 18°C for regeneration. The regeneration index was calculated by

222 summing the product of approximate wing size (0%, 25%, 50%, 75% and 100%)

223 and the corresponding percentage of wings for each wing size. The Δ Index was

224 calculated by subtracting the regeneration index of the control from the regenera-

225 tion index of the mutant or RNAi line.

226

227 To observe and quantify the patterning features and absolute wing size, adult

228 wings that were 75% size or greater were mounted in Gary's Magic Mount (Can-

229 ada balsam (Sigma) dissolved in methyl salicylate (Sigma)). The mounted adult

230 wings were imaged with an Olympus SZX10 microscope using an Olympus

231 DP21 camera, with the Olympus CellSens Dimension software. Wings were

232 measured using ImageJ.

233

234 **Immunostaining**

Immunostaining was carried out as previously described (Smith-Bolton et al., 2009). Primary antibodies used in this study were rabbit anti-Myc (1:500; Santa Cruz Biotechnology), mouse anti-Nubbin (1:250; gift from Steve Cohen) (Ng et al., 1996), mouse anti-engrailed/invected (1:3; Developmental Studies Hybridoma Bank (DSHB)) (Patel et al., 1989), mouse anti-Patched (1:50; DSHB) (Capdevila et al., 1994), mouse anti-Achaete (1:10; DSHB) (Skeath and Carroll, 1992), rabbit anti-PH3 (1:500; Millipore), mouse anti-Osa (1:1; DSHB) (Treisman et al., 1997), rat anti-Ci (1:10; DSHB) (Motzny and Holmgren, 1995), rabbit anti-Dcp1 (1:250; Cell Signaling), mouse anti-βgal (1:100; DSHB), rabbit anti-phospho-Mad (1:100; Cell Signaling), mouse anti-Mmp1 (1:10 of 1:1:1 mixture of monoclonal antibodies 3B8D12, 5H7B11, and 3A6B4, DSHB)(Page-McCaw et al., 2003). The Developmental Studies Hybridoma Bank (DSHB) was created by the NICHD of the NIH and is maintained at the University of Iowa, Department of Biology, Iowa City, IA 52242. Secondary antibodies used in this study were AlexaFluor secondary antibodies (Molecular Probes) (1:1000). TO-PRO-3 iodide (Molecular Probes) was used to detect DNA at 1:500.

Confocal images were collected with a Zeiss LSM700 Confocal Microscope using ZEN software (Zeiss). Images were processed with ImageJ (NIH) and Photoshop (Adobe). Average fluorescence intensity was measured by ImageJ. Quantification of fluorescence intensity and phospho-histone H3 positive cells was restricted to the wing pouch, as marked by anti-Nubbin immunostaining or morphology. The area of the regenerating wing primordium was quantified by measuring the anti-Nubbin immunostained area in ImageJ.

Quantitative RT-PCR

qPCR was conducted as previously described (Skinner et al., 2015). Each independent sample consisted of 50 wing discs. 3 biological replicates were collected for each genotype and time point. Expression levels were normalized to the control *gapdh2*. The fold changes compared to the w^{1118} undamaged wing discs are shown. Primers used in the study were:

GAPDH2 (Forward: 5'-GTGAAGCTGATCTCTTGGTACGAC-3';
Reverse: 5'-CCGCGCCCTAATCTTTAACTTTTAC-3'),
ilp8 (Qiagen QT00510552),
mmp1 (Forward: 5'-TCGGCTGCAAGAACACGCCC-3';
Reverse: 5'-CGCCCACGGCTGCGTCAAAG-3'),
moira (Forward: 5'-GATGAGGTGCCCGCTACAAT-3';
Reverse: 5'-CTGCTGCGGTTTCGTCTTTT-3'),
brm (Forward: 5'-GCACCACCAGGGGATGATTT-3';
Reverse: 5'-TTGTGTGGGTGCATTGGGT-3'),
Bap60 (Forward: 5'-AGACGAGGGATTTGAAGCTGA-3';
Reverse: 5'-AGGTCTCTTGACGGTGGACT-3')
myc (Forward: 5'-CGATCGCAGACGACAGATAA-3';
Reverse: 5'-GGGCGGTATTAAATGGACCT-3')

Pupariation timing experiments

To quantify the pupariation rates, pupal cases on the side of each vial were counted at 24-hour intervals starting from the end of tissue ablation until no new pupal cases formed. Three independent biological replicates, which consisted of 3 vials each with 50 animals per vial, were performed for each experiment. The median day is the day on which ≥ 50% of the animals had pupariated.

Data Availability

All relevant data are available at databank.illinois.edu.XXXXXXXX and upon request.

Results

A genetic screen of chromatin modifier mutants and RNAi lines

To identify regeneration genes among *Drosophila* chromatin regulators, we conducted a genetic screen similar to our previously reported unbiased genetic screen for genes that regulate wing imaginal disc regeneration (Brock et al., 2017)(Fig. 1A). To induce tissue ablation, *rotund-GAL4* drove the expression of the pro-apoptotic gene *UAS-reaper* in the imaginal wing pouch, and *tubulin-GAL80^{ts}* provided temporal control, enabling us to turn ablation on and off by varying the temperature (Smith-Bolton et al., 2009). The ablation was carried out for 24 hours during the early third instar. We characterized the quality of regeneration by assessing the adult wing size semi-quantitatively and 1) recording the numbers of wings that were 0%, 25%, 50%, 75% or 100% the length of a normal adult wing (Fig. 1A,B), and 2) identifying patterning defects by scoring ectopic or missing features. This semi-quantitative evaluation method enabled a quick screen, at a rate of 6 genotypes per week including around 1400 adult wings, and identification of both enhancers and suppressors of regeneration (Fig. 1B-E). While control animals regenerated to varying degrees depending on the extent they delayed metamorphosis in response to damage (Khan et al., 2017; Smith-Bolton et al., 2009) as well as seasonal differences in humidity and food quality (Skinner et al., 2015), the differences between the regenerative capacity of mutants and controls were consistent (Brock et al., 2017; Khan et al., 2017; Smith-Bolton et al., 2009).

Using this system, we screened mutants and RNAi lines affecting chromatin regulators (Table S1, Fig. 1C, Fig. S1A). For each line, we calculated the Δ regeneration index, which is the difference between the regeneration indices of the line being tested and the control tested simultaneously (see materials and methods for regeneration index calculation). We set a cutoff Δ index of 10%, over which we considered the regenerative capacity to be affected. Seventy-eight percent of the mutants and RNAi lines tested had a change in regeneration index of 10% or more compared to controls (Table S1, Fig. 1C, Fig. S1A), consistent with the idea that changes in chromatin structure are required for the damaged tissue to execute the regeneration program. Twenty-two percent of the mutants and RNAi lines failed to meet our cutoff and were not pursued further (Table S1, Fig. 1C). Strikingly, 41% of the tested lines, such as *phol*^{81A}/+, which affects the PhoRC complex, had larger adult wings after ablation and regeneration compared to control *w*^{1118} animals that had also regenerated (Fig. 1D), indicating enhanced regeneration, although none were larger than a normal-sized wing. By contrast, 25% of the tested lines, such as *E(bx)*$^{nurf301-3}$/+, which affects the NURF complex, had smaller wings (Fig. 1E), indicating worse regeneration. Unexpectedly, mutations that affected the same complex did not have consistent phenotypes (Table S1), suggesting that chromatin modification and remodeling likely regulate a delicate balance of genes that promote and constrain regeneration. Indeed, transcriptional profiling has identified a subset of genes that are upregulated after wing disc ablation (Khan et al., 2017), some of which promote regeneration, and some of which constrain regeneration, indicating that gene regulation after tissue damage is not as simple as turning on genes that promote regeneration and turning off genes that inhibit regeneration.

The SWI/SNF PBAP and BAP complexes have opposite phenotypes.

To clarify the roles of one type of chromatin-regulating complex in regeneration, we focused on the SWI/SNF chromatin-remodeling complexes (Fig. 2A). As shown in Table S1, different components of the SWI/SNF complexes showed different phenotypes after ablation and regeneration of the wing pouches. Animals heterozygous mutant for the PBAP-specific components Bap170 (*Bap170*$^{\Delta 135}$/+) and Polybromo (*polybromo*$^{\Delta 86}$/+) had adult wings that were smaller after disc regeneration than *w*^{1118} adult wings after disc regeneration (Fig. 2B,C), suggesting that the PBAP complex is required for ablated wing discs to regrow. To confirm these semiquantitative results, we mounted adult wings and measured absolute wing sizes (N≥100 wings for each genotype). The reduced regeneration of *Bap170*$^{\Delta 135}$/+ wing discs was confirmed by measurement of the adult wings (Fig. 2E). By contrast, animals heterozygous mutant for the BAP-specific component Osa (*osa*^{308}/+) had larger adult wings after disc regeneration compared to *w*^{1118} adult wings after disc regeneration (Fig. 2D), suggesting that impairment of the BAP complex deregulates growth after tissue damage. Measurement of the adult wings of *osa*^{308}/+ animals after disc regeneration confirmed the enhanced regeneration (Fig. 2F).

Interestingly, the *osa*^{308}/+ adult wings also showed severe patterning defects after damage and regeneration of the disc (Fig. 2G-I). Specifically, the posterior compartment of the *osa*^{308}/+ wings had anterior features after wing pouch ablation, but had normal wings when no tissue damage was induced (Fig. S1B). To quantify the extent of the posterior-to-anterior (P-to-A) transformations, we quantified the number of anterior features in the posterior of each wing, including

366 socketed bristles and ectopic veins on the posterior margin, an ectopic anterior
367 crossvein (ACV), costal bristles on the alula, and an altered shape that has a nar-
368 rower proximal and wider distal P compartment (Schuster and Smith-Bolton,
369 2015) (Fig. 2I). While w^{1118} adult wings that had regenerated as discs had a low
370 level of P-to-A transformations, 75% of the osa^{308}/+ wings had P-to-A transfor-
371 mations, and 83% of these transformed wings had 4 or 5 anterior markers in the
372 posterior of the wing. Thus, Osa is required to preserve posterior cell fate during
373 regeneration, suggesting that the BAP complex regulates cell fate after damage.
374
375 **Reducing the core SWI/SNF components to varying levels produces either**
376 **the BAP or PBAP phenotype**
377 Because mutants of the BAP or PBAP complex-specific components showed dis-
378 tinct phenotypes, we also screened mutants of the core components for regener-
379 ation phenotypes. Interestingly, mutants or RNAi lines that reduced levels of the
380 core components were split between the two phenotypes. For example, brm^{2}/+
381 discs and discs expressing a *Bap111* RNAi construct regenerated poorly, result-
382 ing in small wings (Fig. 3A,B), while $Bap55^{LL05955}$/+ discs, mor^{1}/+ discs, and discs
383 expressing a *Bap60* RNAi construct regenerated to produce larger wings overall
384 that showed P-to-A transformations (Table S1, Fig. 3C-G, Fig. S1A).
385
386 Given that the SWI/SNF complexes require the function of the scaffold Mor and
387 the ATPase Brm (Mashtalir et al., 2018; Moshkin et al., 2007), it was surprising
388 that reduction of Mor showed the BAP phenotype while reduction of Brm showed
389 the PBAP phenotype. However, it is likely that some of the mutants and RNAi
390 lines caused stronger loss of function than others. A stronger reduction in func-
391 tion would result in malfunction of both BAP and PBAP, and show the reduced

392 regeneration phenotype, masking any patterning defects. By contrast, a weaker
393 reduction in function could mainly affect the BAP complex. For example, *Bap60*
394 RNAi, which caused patterning defects after wing disc regeneration, only induced
395 a moderate reduction in mRNA levels, suggesting that it causes a weak loss of
396 function (Fig S1C). Although it is unclear why a weaker reduction of function
397 would mainly affect the BAP complex, it is possible that the BAP complex is less
398 abundant than the PBAP complex, such that a slight reduction in a core compo-
399 nent would have a greater effect on the amount of BAP in the tissue. Therefore,
400 we hypothesized that stronger or weaker loss of function of the same core com-
401 plex component might show different phenotypes.
402
403 To test this hypothesis, we used a strong loss-of-function *mor* mutant, mor^{11} (gift
404 from J. Kennison, Fig. S1D), and two hypomorphic *mor* mutants mor^{1} *and* mor^{2}
405 (Kennison and Tamkun, 1988). Indeed, mor^{11}/+ undamaged wing discs had sig-
406 nificantly less *mor* transcript than mor^{1}/+ or control undamaged wing discs (Fig.
407 3H). Interestingly, mor^{11}/+ animals showed the poor regeneration phenotype sim-
408 ilar to the PBAP complex-specific $Bap170^{\Delta 135}$/+ mutants (Fig. 3I), while mor^{1}/+
409 and mor^{2}/+ showed the enhanced regeneration phenotype and the P-to-A trans-
410 formation phenotype similar to the BAP complex-specific osa^{308}/+ mutants (Fig.
411 3E,J, S1Table). To confirm these findings we also used an amorphic allele of *brm*
412 and an RNAi line that targets *brm* to reduce the levels of the core component
413 *brm*. brm^{2} was generated through ethyl methanesulfonate mutagenesis and
414 causes a loss of Brm protein (Elfring et al., 1998; Kennison and Tamkun, 1988).
415 The *brm* RNAi causes a partial reduction in transcript, as *rn>brmRNAi* undam-
416 aged wing discs had less *brm* transcript than control undamaged wing discs (Fig.
417 S1E). brm^{2}/+ animals showed the small wing phenotype after disc damage,

418 indicating poor regeneration (Fig. 3A). By contrast, knockdown of *brm* by ex-
419 pressing the *brm* RNAi construct during tissue ablation induced larger wings and
420 P-to-A transformations (Fig. 3K,L). Thus, slight reduction of the core SWI/SNF
421 components, through mor^{1}, *brm* RNAi, or *Bap60* RNAi, produced the BAP pheno-
422 type, whereas stronger reduction of the core components, through mor^{11}, pro-
423 duced the PBAP phenotype, suggesting that it is easier to compromise BAP
424 function than to compromise PBAP function. If it is easier to compromise BAP
425 function because there is less BAP complex in regenerating wing disc cells, over-
426 expression of the BAP-specific component Osa would lead to an increase in the
427 amount of BAP complex and rescue the *brm* RNAi phenotype. Indeed, overex-
428 pression of *osa* in regenerating tissue rescued the enhanced wing size and P-to-
429 A transformations induced by *brm* RNAi (Fig. 3M,N).
430
431 **The PBAP complex is required for Myc upregulation and cell proliferation**
432 **during regrowth**
433 To identify when the defect in regrowth occurs in PBAP complex mutants, we
434 measured the regenerating wing pouch using expression of the pouch marker
435 *nubbin* in w^{1118} controls, $Bap170^{\Delta 135}$/+ and brm^{2}/+ mutants, as well as in the
436 osa^{308}/+ BAP mutant for comparison. The regenerating wing pouches of
437 $Bap170^{\Delta 135}$/+ mutant animals were not different in size compared to w^{1118} animals
438 at 0, 12, or 24 hours after tissue damage (R0, R12 or R24). However, the
439 $Bap170^{\Delta 135}$/+ regenerating wing pouches were smaller than w^{1118} by 36 hours af-
440 ter tissue damage (R36), shortly before the $Bap170^{\Delta 135}$/+ mutant animals pupari-
441 ated and entered metamorphosis (Fig. 4A-C). brm^{2}/+ mutant animals also had
442 smaller regenerating wing pouches by R24 (Fig. S2A-C). By contrast, the regen-
443 erating osa^{308}/+ wing pouches regrew at the same rate as controls (Fig. S2D-H).

To determine whether the *Bap170*$^{\Delta 135}$/+ mutant animals had a slower rate of proliferation during regeneration, we quantified the number of mitotic cells by immunostaining for phospho-histone H3 (PH3) in the regenerating wing pouch. A 35% decrease in the number of PH3-positive cells was observed in *Bap170*$^{\Delta 135}$/+ mutants (Fig. 4D-F, Fig. S2I). While smaller adult wings could also be caused by increased cell death in the regenerating tissue, we did not find an increase in cell death in *Bap170*$^{\Delta 135}$/+ regenerating wing discs as marked by immunostaining for cleaved caspase Dcp1 (Fig. S2J,K).

To identify why proliferation was reduced in *Bap170*$^{\Delta 135}$/+ mutants, we examined levels of Myc, an important growth regulator that is upregulated during *Drosophila* wing disc regeneration (Smith-Bolton et al., 2009). In mammals, *c-myc* is a direct target of the SWI/SNF BAF complex, which is similar to *Drosophila* BAP (Nagl et al., 2006), but a role for the PBAP complex in regulating the *Drosophila Myc* gene has not been established. Myc protein levels were significantly reduced in *Bap170*$^{\Delta 135}$/+ and *brm*^{2}/+ regenerating wing pouches compared to wild-type regenerating wing pouches (Fig. 4G-I and Fig. S3A-D). Myc transcriptional levels were also significantly lower in *Bap170*$^{\Delta 135}$/+ regenerating wing discs compared to wild-type regenerating discs (Fig. 4J). By contrast, there was no change in Myc levels in *osa*^{308}/+ mutants (Fig. S3E-G), indicating that PBAP, but not BAP, is required for upregulation of Myc after tissue damage. To determine the extent to which reduction of Myc expression was responsible for the poor regeneration phenotype in BAP complex mutants, we overexpressed Myc in the *Bap170*$^{\Delta 135}$/+ background during regeneration. Indeed, the *Bap170*$^{\Delta 135}$/+, *UAS-Myc*/+ animals regenerated similar to the *w*^{1118} controls and significantly better

than *Bap170*$^{\Delta 135}$/+ animals, demonstrating partial rescue of the poor regeneration phenotype (Fig. 4K and Fig. S3H).

The PBAP complex is required for the delay in pupariation induced by tissue damage

Damaged imaginal discs delay pupariation by expressing the peptide ILP8, which delays the production of ecdysone and onset of metamorphosis, providing more time for damaged tissue to regenerate (Colombani et al., 2012; Garelli et al., 2012). To determine whether the SWI/SNF complexes regulate the timing of metamorphosis, we quantified the pupariation rate in *w*^{1118} and *Bap170*$^{\Delta 135}$/+ regenerating animals, and identified the day on which 50% of the larvae had pupariated. Without tissue damage, *Bap170*$^{\Delta 135}$/+ mutants pupariated slightly later than *w*^{1118} animals (Fig. 4L and Fig. S4A), but the difference is not significant. However, after wing disc damage, more than half of the *Bap170*$^{\Delta 135}$/+ mutant animals had pupariated by 2 days after damage, whereas more than half of the *w*^{1118} animals had not pupariated until 3 days after damage, giving the mutants 1/3 less time to regenerate (Fig. 4M and Fig. S4B). To uncover why *Bap170*$^{\Delta 135}$/+ animals had less regeneration time, we quantified *ilp8* transcript levels. Indeed, *Bap170*$^{\Delta 135}$/+ animals had about 50% less *ilp8* mRNA (Fig. 4N), suggesting that the PBAP complex is required for *ilp8* expression.

The PBAP complex regulates expression of JNK signaling targets

SWI/SNF complexes can be recruited by transcription factors to act as co-activators of gene expression (Becker and Workman, 2013). Regenerative growth and the pupariation delay are regulated by JNK signaling (Bergantinos et al., 2010; Bosch et al., 2008; Colombani et al., 2012; Garelli et al., 2012; Skinner et al.,

2015). Thus, it is possible that PBAP is recruited to JNK signaling targets like *ilp8* by the AP-1 transcription factor, which acts downstream of JNK (Perkins et al., 1988), and that PBAP is required for full activation of these targets. To determine whether *Bap170* is required for JNK-dependent transcription, we examined the activity of the TRE-Red reporter, which is comprised of four AP-1 binding sites (TREs) driving the expression of a DsRed.T4 reporter gene (Chatterjee and Bohmann, 2012) in w^{1118} and $Bap170^{\Delta 135}$/+ regenerating wing discs. The TRE-Red intensity was significantly decreased in the $Bap170^{\Delta 135}$/+ regenerating tissue compared to the w^{1118} regenerating tissue (Fig. 4O-R), indicating that PBAP is required for full activation of this AP-1 transcriptional activity reporter, similar to its requirement for expression of *ilp8*. Furthermore, expression of the JNK signaling target *mmp1* was significantly reduced in $Bap170^{\Delta 135}$/+ regenerating wing discs at both the mRNA and protein levels (Fig. 4S and Fig. S4C-E). Thus, the PBAP complex plays a crucial role in activation of JNK signaling targets.

The BAP complex maintains posterior cell fate during regeneration

After damage and regeneration of the disc, adult wings of osa^{308}/+, $Bap55^{LL05955}$/+, mor^{1}/+, and mor^{2}/+ discs, as well as discs expressing a *brm* RNAi construct or a *Bap60* RNAi construct, had anterior bristles and veins in the posterior compartment (Fig. 3C-G,K), but not after normal development (Fig. S1A, S1F-H). To identify when the P-to-A transformations occurred, we examined the expression of anterior- and posterior-specific genes during tissue regeneration. *engrailed* (*en*) is essential for posterior cell fate both in development and regeneration (Kornberg et al., 1985; Schuster and Smith-Bolton, 2015). To assess ability to maintain posterior cell fate, regenerating wing discs were dissected at different times during recovery (R) and immunostained for the posterior selector

gene *en*. At 72 hours after damage (R72), in osa^{308}/+ regenerating discs, *en* was expressed in some of the posterior compartment, but lost in patches (Fig. 5A-C). In addition, the proneural protein Acheate (Ac), which is expressed in sensory organ precursors in the anterior of wing discs (Skeath and Carroll, 1991), was ectopically expressed in the posterior (Fig. 5D-F) marking precursors to the ectopic socketed bristles found in the posterior of the adult wings. The anterior genes *cubitus interruptus* (*ci*) (Eaton and Kornberg, 1990) and *patched* (*ptc*) (Phillips et al., 1990) were also ectopically expressed in the posterior of the osa^{308}/+ R72 regenerating wing discs (Fig. 6A-C). The ectopic expression of these anterior genes was not observed at R48, suggesting that the P-to-A fate transformations happened late during regeneration (Fig. S4F,G). Similarly, at R72, 80% of the *brm* RNAi wing discs had ectopic expression of the anterior genes *ptc* and *ci* in the posterior of the discs, while no expression of *ptc* or *ci* was observed in the posterior of control R72 discs (Fig. 6D,E).

We previously showed that in *Drosophila* wing disc regeneration, elevated JNK increases expression of *en*, leading to PRC2-mediated silencing of the *en* locus in patches, and transformation of the *en*-silenced cells to anterior fate, and that Taranis prevents this misregulation of *en* and resulting P-to-A cell fate transformations (Schuster and Smith-Bolton, 2015). Thus, we wondered whether the BAP complex preserved *en* expression and posterior fate by reducing JNK signaling, or regulating *tara* expression, or working in parallel to Tara during the later stages of regeneration.

The BAP complex does not regulate JNK signaling

To determine whether the BAP complex regulates JNK signaling, we examined the JNK reporter TRE-Red in *osa*^{308}/+ and *w*^{1118} regenerating wing discs. In contrast to *Bap170*$^{\Delta 135}$/+ mutants (Fig. 4O-R), TRE-Red intensity was not different between *osa*^{308}/+ and *w*^{1118} regenerating tissue (Fig. 7A-C). Thus, the BAP complex acts to protect posterior cell fate downstream of or in parallel to JNK signaling.

The BAP complex functions in parallel to Taranis to preserve cell fate

Because *tara* is regulated transcriptionally after tissue damage (Schuster and Smith-Bolton, 2015), we examined whether the BAP complex is required for *tara* upregulation in the regenerating tissue. Using a *tara-lacZ* enhancer trap, we assessed expression in *Bap55*^{LL05955}/+ regenerating wing discs, which had the same P-to-A transformations as the *osa*^{308}/+ regenerating discs. No change in *tara-lacZ* expression was identified in the regenerating wing pouches, (Fig. 7D-G), indicating that the damage-dependent *tara* expression was not downstream of BAP activity.

To determine whether Tara can suppress the P-to-A transformations induced by the reduction of BAP, we overexpressed Tara using *UAS-tara* under control of *rn-Gal4* in the *osa*^{308}/+ mutant animals, generating elevated Tara levels in the *rn*-expressing cells that survived the tissue ablation. Indeed, the P-to-A transformation phenotype in *osa*^{308}/+ mutant animals was rescued by Tara overexpression (Fig. 7H-K). To rule out the possibility that Tara regulates *osa* expression, we quantified Osa immunostaining in *tara/+* mutant regenerating tissue. Osa protein levels did not change during regeneration, and were unchanged in *tara*^{1}/+ mutant regenerating discs (Fig. S4H-M). Taken together, these data indicate that the BAP

573 complex likely functions in parallel to Tara to constrain *en* expression, preventing
574 auto-regulation and silencing of *en*, thereby protecting cell fate from changes in-
575 duced by JNK signaling during regeneration.
576
577 **The enhanced growth in BAP mutants is caused by ectopic AP boundaries.**
578 The increased wing size after disc regeneration in *tara/+* animals was due to loss
579 of *en* in patches of cells, which generated aberrant juxtaposition of anterior and
580 posterior tissue within the posterior compartment. These ectopic AP boundaries
581 established ectopic Dpp morphogen gradients (Schuster and Smith-Bolton,
582 2015), which can stimulate extra growth in the posterior compartment (Tanimoto
583 et al., 2000). To determine whether the *osa/+* regenerating discs also had ectopic
584 AP boundaries and ectopic morphogen gradients, we immunostained for Ptc to
585 mark AP boundaries and phospho-Smad to visualize gradients of Dpp signaling.
586 Indeed, Ectopic regions of Ptc expression were surrounded by ectopic pSmad
587 gradients in osa^{308}/+ regenerating discs (Fig. 8A-C). Thus, the enhanced regen-
588 eration in osa^{308}/+ and other SWI/SNF mutant animals was likely a secondary re-
589 sult of the patterning defect. Furthermore, pupariation occurred later in osa^{308}/+
590 regenerating animals compared to w^{1118} regenerating animals (Fig. S4N,O),
591 which provided more time for regeneration in the mutants. Such a delay in pupar-
592 iation can by caused by aberrant proliferation (Colombani et al., 2012; Garelli et
593 al., 2012) in addition to tissue damage, and the combination of the two likely led
594 to the increase in delay in metamorphosis seen specifically in mutants with P-to-
595 A transformations.
596
597 **Discussion**

598 To address the question of how regeneration genes are regulated in response to
599 tissue damage, we screened a collection of mutants and RNAi lines that affect a
600 significant number of the chromatin regulators in *Drosophila*. Most of these mu-
601 tants had regeneration phenotypes, confirming that these genes are important for
602 both promoting and constraining regeneration and likely facilitate the shift from
603 the normal developmental program to the regeneration program, and back again.
604 The variation in regeneration phenotypes among different chromatin regulators
605 and among components of the same multi-unit complexes supports our previous
606 finding that damage activates expression of genes that both promote and con-
607 strain regeneration (Khan et al., 2017). Such regulators of regeneration may be
608 differentially affected by distinct mutations that affect the same chromatin-modify-
609 ing complexes, resulting in different phenotypes.
610
611 We have demonstrated that both *Drosophila* SWI/SNF complexes play essential
612 but distinct roles during epithelial regeneration, controlling multiple aspects of the
613 process, including growth, developmental timing, and cell fate (Fig. 8D). Further-
614 more, our work has identified multiple likely targets, including *mmp1, myc*, *ilp8*,
615 and *en*. Indeed, analysis of data from a recent study that identified regions of the
616 genome that transition to open chromatin after imaginal disc damage showed
617 such damage-responsive regions near *Myc*, *mmp1*, and *ilp8* (Vizcaya-Molina et
618 al., 2018). While previous work has suggested that chromatin modifiers can regu-
619 late regeneration (Blanco et al., 2010; Fukuda et al., 2012; Jin et al., 2013; Jin et
620 al., 2015; Pfefferli et al., 2014; Scimone et al., 2010; Skinner et al., 2015; Stewart
621 et al., 2009; Sun et al., 2016; Tseng et al., 2011; Wang et al., 2008; Xiong et al.,
622 2013), and that the chromatin near *Drosophila* regeneration genes is modified af-
623 ter damage (Harris et al., 2016; Vizcaya-Molina et al., 2018), our results suggest

that these damage-responsive loci are not all coordinately regulated in the same manner. The SWI/SNF complexes target different subsets of genes, and it will not be surprising if different cofactors or transcription factors recruit different complexes to other subsets of regeneration genes.

Is the requirement for the SWI/SNF complexes for growth and conservation of cell fate in the wing disc specific to regeneration? In contrast to *tara,* which is required for posterior wing fate only after damage and regeneration (Schuster and Smith-Bolton, 2015), loss of *mor* in homozygous clones during wing disc development caused loss of *en* expression in the posterior compartment (Brizuela and Kennison, 1997), although this result was interpreted to mean that *mor* promotes rather than constrains *en* expression, which is the opposite of our observations. Importantly, undamaged *mor* heterozygous mutant animals did not show patterning defects (Fig. S1G,H), while damaged heterozygous mutant animals did (Fig. 3E), indicating that regenerating tissue is more sensitive to reductions in SWI/SNF levels than normally developing tissue. Furthermore, *osa* is required for normal wing growth (Terriente-Félix and de Celis, 2009), but reduction of *osa* levels did not compromise growth during regeneration (Fig. 2D). Thus, while some functions of SWI/SNF during regeneration may be the same as during development, other functions of SWI/SNF are unique to regeneration.

SWI/SNF complexes help organisms respond rapidly to stressful conditions or changes in the environment. For example, SWI/SNF is recruited by the transcription factor DAF-16/FOXO to promote stress resistance in *Caenorhabditis elegans* (Riedel et al., 2013), and the *Drosophila* BAP complex is required for the activation of target genes of the NF-κB signaling transcription factor Relish in immune

650 responses (Bonnay et al., 2014). Here we show that the *Drosophila* PBAP com-
651 plex is similarly required after tissue damage for activation of target genes of the
652 JNK signaling transcription factor AP-1 after tissue damage. Interestingly, the
653 BAF60a subunit, a mammalian homolog of *Drosophila* BAP60, directly binds the
654 AP-1 transcription factor and stimulates the DNA-binding activity of AP-1 (Ito et
655 al., 2001), suggesting that this role may be conserved.
656
657 In summary, we have demonstrated that the two SWI/SNF complexes regulate
658 different aspects of wing imaginal disc regeneration, implying that activation of
659 the regeneration program is controlled by changes in chromatin, but that the
660 mechanism of regulation is likely different for subsets of regeneration genes. Fu-
661 ture identification of all genes targeted by BAP and PBAP after tissue damage,
662 the factors that recruit these chromatin-remodeling complexes, and the changes
663 they induce at these loci will deepen our understanding of how unexpected or
664 stressful conditions lead to rapid activation of the appropriate genes.
665
666 **Acknowledgements**
667 The authors would like to thank A. Brock and K. Schuster for critical reading of
668 the manuscript and helpful discussions; A. Dingwall, D. Bohmann, J. Kennison, J.
669 Treisman, M Cleary, S. Cohen, the Bloomington Drosophila Stock Center (NIH
670 P40OD018537), the Vienna *Drosophila* Resource Center, and the Developmen-
671 tal Studies Hybridoma Bank for fly stocks and reagents.
672
673 **Competing interests**
674 No competing interests declared.
675

Funding Sources

This work was supported by a Young Investigator Award from the Roy J. Carver Charitable Trust (#12-4041) (https://www.carvertrust.org) and a grant from the Nation Institutes of Health (NIGMS R01GM107140) (https://www.nigms.nih.gov).

References

Becker, P. B. and Workman, J. L. (2013). Nucleosome Remodeling and Epigenetics. *Cold Spring Harb. Perspect. Biol.* **5**, a017905–a017905.

Bergantinos, C., Corominas, M. and Serras, F. (2010). Cell death-induced regeneration in wing imaginal discs requires JNK signalling. *Development* **137**, 1169–1179.

Blanco, E., Ruiz-Romero, M., Beltran, S., Bosch, M., Punset, A., Serras, F. and Corominas, M. (2010). Gene expression following induction of regeneration in Drosophila wing imaginal discs. Expression profile of regenerating wing discs. *BMC Dev. Biol.* **10**, 94.

Bonnay, F., Nguyen, X.-H., Cohen-Berros, E., Troxler, L., Batsche, E., Camonis, J., Takeuchi, O., Reichhart, J.-M. and Matt, N. (2014). Akirin specifies NF- B selectivity of Drosophila innate immune response via chromatin remodeling. *EMBO J.* **33**, 2349–2362.

Bosch, M., Bagun, J. and Serras, F. (2008). Origin and proliferation of blastema cells during regeneration of Drosophila wing imaginal discs. *Int. J. Dev. Biol.* **52**, 1043–1050.

Brizuela, B. J. and Kennison, J. A. (1997). The Drosophila homeotic gene moira regulates expression of engrailed and HOM genes in imaginal tissues. *Mech. Dev.* **65**, 209–220.

Brock, A. R., Seto, M. and Smith-Bolton, R. K. (2017). Cap-n-collar Promotes Tissue Regeneration by Regulating ROS and JNK Signaling in the *Drosophila* Wing Imaginal Disc. *Genetics* **206**, 1505–1520.

Capdevila, J., Estrada, M. P., Sánchez-Herrero, E. and Guerrero, I. (1994). The Drosophila segment polarity gene patched interacts with decapentaplegic

in wing development. *EMBO J.* **13**, 71–82.

Carrera, I., Zavadil, J. and Treisman, J. E. (2008). Two Subunits Specific to the PBAP Chromatin Remodeling Complex Have Distinct and Redundant Functions during Drosophila Development. *Mol. Cell. Biol.* **28**, 5238–5250.

Chalkley, G. E., Moshkin, Y. M., Langenberg, K., Bezstarosti, K., Blastyak, A., Gyurkovics, H., Demmers, J. A. A. and Verrijzer, C. P. (2008). The Transcriptional Coactivator SAYP Is a Trithorax Group Signature Subunit of the PBAP Chromatin Remodeling Complex. *Mol. Cell. Biol.* **28**, 2920–2929.

Chatterjee, N. and Bohmann, D. (2012). A Versatile ΦC31 Based Reporter System for Measuring AP-1 and Nrf2 Signaling in Drosophila and in Tissue Culture. *PLoS ONE* **7**, e34063.

Collins, R. T. and Treisman, J. E. (2000). Osa-containing Brahma chromatin remodeling complexes are required for the repression of wingless target genes. *Genes Dev.* **14**, 3140–3152.

Collins, R. T., Furukawa, T., Tanese, N. and Treisman, J. E. (1999). Osa associates with the Brahma chromatin remodeling complex and promotes the activation of some target genes. *EMBO J.* **18**, 7029–7040.

Colombani, J., Andersen, D. S. and Léopold, P. (2012). Secreted Peptide Dilp8 Coordinates Drosophila Tissue Growth with Developmental Timing. *Science* **336**, 582–585.

Côté, J., Quinn, J., Workman, J. L. and Peterson, C. L. (1994). Stimulation of GAL4 derivative binding to nucleosomal DNA by the yeast SWI/SNF complex. *Science* **265**, 53–60.

Eaton, S. and Kornberg, T. B. (1990). Repression of ci-D in posterior compartments of Drosophila by engrailed. *Genes Dev.* **4**, 1068–1077.

Elfring, L. K., Daniel, C., Papoulas, O., Deuring, R., Sarte, M., Moseley, S., Beek, S. J., Waldrip, W. R., Daubresse, G., DePace, A., et al. (1998). Genetic analysis of brahma: the Drosophila homolog of the yeast chromatin remodeling factor SWI2/SNF2. *Genetics* **148**, 251–265.

Fukuda, A., Morris, J. P. and Hebrok, M. (2012). Bmi1 Is Required for Regeneration of the Exocrine Pancreas in Mice. *Gastroenterology* **143**, 821–831.e2.

Garelli, A., Gontijo, A. M., Miguela, V., Caparros, E. and Dominguez, M. (2012). Imaginal Discs Secrete Insulin-Like Peptide 8 to Mediate Plasticity of Growth and Maturation. *Science* **336**, 579–582.

Grusche, F. A., Degoutin, J. L., Richardson, H. E. and Harvey, K. F. (2011). The Salvador/Warts/Hippo pathway controls regenerative tissue growth in Drosophila melanogaster. *Dev. Biol.* **350**, 255–266.

Gutierrez, L. (2003). The Drosophila trithorax group gene tonalli(tna) interacts genetically with the Brahma remodeling complex and encodes an SP-RING finger protein. *Development* **130**, 343–354.

Hargreaves, D. C. and Crabtree, G. R. (2011). ATP-dependent chromatin remodeling: genetics, genomics and mechanisms. *Cell Res.* **21**, 396–420.

Hariharan, I. K. and Serras, F. (2017). Imaginal disc regeneration takes flight. *Curr. Opin. Cell Biol.* **48**, 10–16.

Harris, R. E., Setiawan, L., Saul, J. and Hariharan, I. K. (2016). Localized epigenetic silencing of a damage-activated WNT enhancer limits regeneration in mature Drosophila imaginal discs. *Elife* **5**, e11588.

Ito, T., Yamauchi, M., Nishina, M., Yamamichi, N., Mizutani, T., Ui, M., Murakami, M. and Iba, H. (2001). Identification of SWI·SNF Complex Subunit BAF60a as a Determinant of the Transactivation Potential of Fos/Jun Dimers. *J. Biol. Chem.* **276**, 2852–2857.

Jin, Y., Xu, J., Yin, M.-X., Lu, Y., Hu, L., Li, P., Zhang, P., Yuan, Z., Ho, M. S., Ji, H., et al. (2013). Brahma is essential for Drosophila intestinal stem cell proliferation and regulated by Hippo signaling. *Elife* **2**, e00999.

Jin, J., Hong, I.-H., Lewis, K., Iakova, P., Breaux, M., Jiang, Y., Sullivan, E., Jawanmardi, N., Timchenko, L. and Timchenko, N. A. (2015). Cooperation of C/EBP family proteins and chromatin remodeling proteins is essential for termination of liver regeneration. *Hepatology* **61**, 315–325.

Kassis, J. A., Kennison, J. A. and Tamkun, J. W. (2017). Polycomb and Trithorax Group Genes in *Drosophila*. *Genetics* **206**, 1699–1725.

Katsuyama, T., Comoglio, F., Seimiya, M., Cabuy, E. and Paro, R. (2015). During Drosophila disc regeneration, JAK/STAT coordinates cell proliferation with Dilp8-mediated developmental delay. *Proc. Natl. Acad. Sci.* **112**,

E2327–E2336.

Kennison, J. A. and Tamkun, J. W. (1988). Dosage-dependent modifiers of polycomb and antennapedia mutations in Drosophila. *Proc. Natl. Acad. Sci.* **85**, 8136–8140.

Khan, S. J., Abidi, S. N. F., Skinner, A., Tian, Y. and Smith-Bolton, R. K. (2017). The Drosophila Duox maturation factor is a key component of a positive feedback loop that sustains regeneration signaling. *PLOS Genet.* **13**, e1006937.

Kornberg, T., Sidén, I., O'Farrell, P. and Simon, M. (1985). The engrailed locus of drosophila: In situ localization of transcripts reveals compartment-specific expression. *Cell* **40**, 45–53.

Kwon, H., Imbalzano, A. N., Khavari, P. A., Kingston, R. E. and Green, M. R. (1994). Nucleosome disruption and enhancement of activator binding by a human SW1/SNF complex. *Nature* **370**, 477–481.

Manansala, M. C., Min, S. and Cleary, M. D. (2013). The Drosophila SERTAD protein Taranis determines lineage-specific neural progenitor proliferation patterns. *Dev. Biol.* **376**, 150–162.

Mashtalir, N., D'Avino, A. R., Michel, B. C., Luo, J., Pan, J., Otto, J. E., Zullow, H. J., McKenzie, Z. M., Kubiak, R. L., St. Pierre, R., et al. (2018). Modular Organization and Assembly of SWI/SNF Family Chromatin Remodeling Complexes. *Cell* **175**, 1272–1288.e20.

Mohrmann, L., Langenberg, K., Krijgsveld, J., Kal, A. J., Heck, A. J. R. and Verrijzer, C. P. (2004). Differential Targeting of Two Distinct SWI/SNF-Related Drosophila Chromatin-Remodeling Complexes. *Mol. Cell. Biol.* **24**, 3077–3088.

Moshkin, Y. M., Mohrmann, L., van Ijcken, W. F. J. and Verrijzer, C. P. (2007). Functional differentiation of SWI/SNF remodelers in transcription and cell cycle control. *Mol. Cell. Biol.* **27**, 651–661.

Motzny, C. K. and Holmgren, R. (1995). The Drosophila cubitus interruptus protein and its role in the wingless and hedgehog signal transduction pathways. *Mech. Dev.* **52**, 137–150.

Nagl, N. G., Zweitzig, D. R., Thimmapaya, B., Beck, G. R. and Moran, E. (2006).

The *c-myc* Gene Is a Direct Target of Mammalian SWI/SNF–Related Complexes during Differentiation-Associated Cell Cycle Arrest. *Cancer Res.* **66**, 1289–1293.

Ng, M., Diaz-Benjumea, F. J., Vincent, J.-P., Wu, J. and Cohen, S. M. (1996). Specification of the wing by localized expression of wingless protein. *Nature* **381**, 316–318.

Page-McCaw, A., Serano, J., Santé, J. M. and Rubin, G. M. (2003). Drosophila matrix metalloproteinases are required for tissue remodeling, but not embryonic development. *Dev. Cell* **4**, 95–106.

Patel, N. H., Martin-Blanco, E., Coleman, K. G., Poole, S. J., Ellis, M. C., Kornberg, T. B. and Goodman, C. S. (1989). Expression of engrailed proteins in arthropods, annelids, and chordates. *Cell* **58**, 955–968.

Perkins, K. K., Dailey, G. M. and Tjian, R. (1988). Novel Jun-and Fos-related proteins in Drosophila are functionally homologous to enhancer factor AP-1. *EMBO J.* **7**, 4265.

Pfefferli, C., Müller, F., Jaźwińska, A. and Wicky, C. (2014). Specific NuRD components are required for fin regeneration in zebrafish. *BMC Biol.* **12**, 1.

Phillips, R. G., Roberts, I. J., Ingham, P. W. and Whittle, J. R. (1990). The Drosophila segment polarity gene patched is involved in a position-signalling mechanism in imaginal discs. *Development* **110**, 105–114.

Riedel, C. G., Dowen, R. H., Lourenco, G. F., Kirienko, N. V., Heimbucher, T., West, J. A., Bowman, S. K., Kingston, R. E., Dillin, A., Asara, J. M., et al. (2013). DAF-16 employs the chromatin remodeller SWI/SNF to promote stress resistance and longevity. *Nat. Cell Biol.* **15**, 491–501.

Santabárbara-Ruiz, P., López-Santillán, M., Martínez-Rodríguez, I., Binagui-Casas, A., Pérez, L., Milán, M., Corominas, M. and Serras, F. (2015). ROS-Induced JNK and p38 Signaling Is Required for Unpaired Cytokine Activation during Drosophila Regeneration. *PLOS Genet.* **11**, e1005595.

Schubiger, M., Sustar, A. and Schubiger, G. (2010). Regeneration and transdetermination: the role of wingless and its regulation. *Dev. Biol.* **347**, 315–324.

Schuldiner, O., Berdnik, D., Levy, J. M., Wu, J. S., Luginbuhl, D., Gontang, A.

C. and Luo, L. (2008). piggyBac-Based Mosaic Screen Identifies a Postmitotic Function for Cohesin in Regulating Developmental Axon Pruning. *Dev. Cell* **14**, 227–238.

Schuster, K. J. and Smith-Bolton, R. K. (2015). Taranis Protects Regenerating Tissue from Fate Changes Induced by the Wound Response in Drosophila. *Dev. Cell* **34**, 119–128.

Scimone, M. L., Meisel, J. and Reddien, P. W. (2010). The Mi-2-like Smed-CHD4 gene is required for stem cell differentiation in the planarian Schmidtea mediterranea. *Development* **137**, 1231–1241.

Skeath, J. B. and Carroll, S. B. (1991). Regulation of achaete-scute gene expression and sensory organ pattern formation in the Drosophila wing. *Genes Dev.* **5**, 984–995.

Skeath, J. B. and Carroll, S. B. (1992). Regulation of proneural gene expression and cell fate during neuroblast segregation in the Drosophila embryo. *Dev. Camb. Engl.* **114**, 939–946.

Skinner, A., Khan, S. J. and Smith-Bolton, R. K. (2015). Trithorax regulates systemic signaling during *Drosophila* imaginal disc regeneration. *Development* **142**, 3500–3511.

Smith-Bolton, R. K., Worley, M. I., Kanda, H. and Hariharan, I. K. (2009). Regenerative Growth in Drosophila Imaginal Discs Is Regulated by Wingless and Myc. *Dev. Cell* **16**, 797–809.

Stewart, S., Tsun, Z.-Y. and Izpisua Belmonte, J. C. (2009). A histone demethylase is necessary for regeneration in zebrafish. *Proc. Natl. Acad. Sci. U. S. A.* **106**, 19889–19894.

Sun, G. and Irvine, K. D. (2011). Regulation of Hippo signaling by Jun kinase signaling during compensatory cell proliferation and regeneration, and in neoplastic tumors. *Dev. Biol.* **350**, 139–151.

Sun, X., Chuang, J.-C., Kanchwala, M., Wu, L., Celen, C., Li, L., Liang, H., Zhang, S., Maples, T., Nguyen, L. H., et al. (2016). Suppression of the SWI/SNF Component Arid1a Promotes Mammalian Regeneration. *Cell Stem Cell* **18**, 456–466.

Tamkun, J. W., Deuring, R., Scott, M. P., Kissinger, M., Pattatucci, A. M.,

Kaufman, T. C. and Kennison, J. A. (1992). brahma: a regulator of Drosophila homeotic genes structurally related to the yeast transcriptional activator SNF2SWI2. *Cell* **68**, 561–572.

Tanimoto, H., Itoh, S., ten Dijke, P. and Tabata, T. (2000). Hedgehog creates a gradient of DPP activity in Drosophila wing imaginal discs. *Mol. Cell* **5**, 59–71.

Terriente-Félix, A. and de Celis, J. F. (2009). Osa, a subunit of the BAP chromatin-remodelling complex, participates in the regulation of gene expression in response to EGFR signalling in the Drosophila wing. *Dev. Biol.* **329**, 350–361.

Treisman, J. E., Luk, A., Rubin, G. M. and Heberlein, U. (1997). eyelidantagonizes wingless signaling during Drosophiladevelopment and has homology to the Bright family of DNA-binding proteins. *Genes Dev.* **11**, 1949–1962.

Tseng, A.-S., Carneiro, K., Lemire, J. M. and Levin, M. (2011). HDAC Activity Is Required during Xenopus Tail Regeneration. *PLOS ONE* **6**, e26382.

Vázquez, M., Moore, L. and Kennison, J. A. (1999). The trithorax group gene osa encodes an ARID-domain protein that genetically interacts with the brahma chromatin-remodeling factor to regulate transcription. *Development* **126**, 733–742.

Vizcaya-Molina, E., Klein, C. C., Serras, F., Mishra, R. K., Guigó, R. and Corominas, M. (2018). Damage-responsive elements in *Drosophila* regeneration. *Genome Res.* **28**, 1852–1866.

Wang, G.-L., Salisbury, E., Shi, X., Timchenko, L., Medrano, E. E. and Timchenko, N. A. (2008). HDAC1 cooperates with C/EBPalpha in the inhibition of liver proliferation in old mice. *J. Biol. Chem.* **283**, 26169–26178.

Wilson, B. G. and Roberts, C. W. M. (2011). SWI/SNF nucleosome remodellers and cancer. *Nat. Rev. Cancer* **11**, 481–492.

Xiong, Y., Li, W., Shang, C., Chen, R. M., Han, P., Yang, J., Stankunas, K., Wu, B., Pan, M., Zhou, B., et al. (2013). Brg1 Governs a Positive Feedback Circuit in the Hair Follicle for Tissue Regeneration and Repair. *Dev. Cell* **25**, 169–181.

Zraly, C. B., Marenda, D. R., Nanchal, R., Cavalli, G., Muchardt, C. and

Dingwall, A. K. (2003). SNR1 is an essential subunit in a subset of Drosophila brm complexes, targeting specific functions during development. *Dev. Biol.* **253**, 291–308.

Fig 1. A genetic screen of chromatin regulators identified important regeneration genes

(A) Method for screening mutants or RNAi lines using a genetic ablation system. Mutants or RNAi lines of genes involved in regulating chromatin were crossed to the ablation stock (*w^{1118}; +; rn-GAL4, UAS-rpr, tubGAL80^{ts}/TM6B, tubGAL80*). Animals were kept at 18°C until 7 days after egg lay (AEL), when they were moved to 30°C to induce tissue ablation for 24 hours, then transferred back to 18°C to enable recovery (R). The size of the regenerated adult wings was assessed semi-quantitatively by counting the number of wings that were approximately 0%, 25%, 50%, 75% or 100% of the length of a control adult wing that had not undergone damage during the larval phase. The regenerating discs were also examined at different times denoted by hours after the beginning of recovery, such as R0, R24, R48 and R72.

(B) Conceptual model for the screen to identify mutants or RNAi lines showing enhanced (green) or reduced (purple) regeneration compared to control.

(C) Summary of the screen of chromatin regulators, showing percent of lines tested that had a regeneration phenotype, as well as percent of those with a phenotype that regenerated better (Δ Index $\geq$ 10%) or worse (Δ Index $\leq$ -10%) compared to controls.

(D) Comparison of the size of adult wings after imaginal disc damage and regeneration in *phol*^{81A}/+ and wild-type (*w*^{1118}) animals. n = 64 wings (*phol*^{81A}/+) and 242 wings (*w*^{1118}) from 3 independent experiments. Chi-square test p < 0.001 across all wing sizes. Error bars are s.e.m.

(E) Comparison of the size of adult wings after imaginal disc damage and regeneration in *E(bx)*$^{nurf301-3}$/+ and wild-type (*w*^{1118}) animals. n = 219 wings (*E(bx)*$^{nurf301-3}$/+) and 295 wings (*w*^{1118}) from 3 independent experiments. Chi-square test p < 0.001 across all wing sizes. Error bars are s.e.m.

Fig 2. SWI/SNF components Bap170, Polybromo and Osa are required for regeneration

(A) Schematics of the two *Drosophila* SWI/SNF chromatin-remodeling complexes: BAP and PBAP, drawn based on complex organization determined in (Mashtalir et al., 2018).

(B) Comparison of the size of adult wings after imaginal disc damage and regeneration in *Bap170*$^{\Delta 135}$/+ and wild-type (*w*^{1118}) animals. n = 190 wings (*Bap170*$^{\Delta 135}$/+) and 406 wings (*w*^{1118}) from 3 independent experiments. Chi-square test p < 0.001 across all wing sizes.

(C) Comparison of the size of adult wings after imaginal disc damage and regeneration in *polybromo*$^{\Delta 86}$/+ and wild-type (*w*^{1118}) animals. n = 180 wings (*polybromo*$^{\Delta 86}$/+) and 396 wings (*w*^{1118}) from 3 independent experiments. Chi-square test p < 0.001 across all wing sizes.

(D) Comparison of the size of adult wings after imaginal disc damage and regeneration in *osa*^{308}/+ and wild-type (*w*^{1118}) animals. n = 146 wings (*osa*^{308}/+) and 296 wings (*w*^{1118}) from three independent experiments. Chi-square test p < 0.001 across all wing sizes.

953 (E) Wings were mounted, imaged, and measured after imaginal disc damage and
954 regeneration in *Bap170*$^{\Delta 135}$/+ and wild-type (*w*^{1118}) animals. n = 100 wings
955 (*Bap170*$^{\Delta 135}$/+) and 224 wings (*w*^{1118}) from 3 independent experiments. Student's
956 t-test, p<0.001
957 (F) Wings were mounted, imaged, and measured after imaginal disc damage and
958 regeneration in *osa*^{308}/+ and wild-type (*w*^{1118}) animals. n = 142 wings (*osa*^{308}/+)
959 and 284 wings (*w*^{1118}) from three independent experiments.
960 (G) Wild-type (*w*^{1118}) adult wing after disc regeneration. Anterior is up.
961 (H) *osa*^{308}/+ adult wing after disc regeneration. Arrows show five anterior-specific
962 markers in the posterior compartment: anterior crossveins (red), alula-like costa
963 bristles (orange), margin vein (green), socketed bristles (blue), and change of
964 wing shape with wider distal portion of the wing, similar to the anterior compart-
965 ment (purple).
966 (I) Quantification of the number of Posterior-to-Anterior transformation markers
967 described in (H) in each wing after damage and regeneration of the disc, using
968 wings that were 75% normal size or larger, comparing *osa*^{308}/+ wings to wild-type
969 (*w*^{1118}) wings, n = 51 wings (*osa*^{308}/+) and 45 wings (*w*^{1118}), from 3 independent
970 experiments. Chi-square test p < 0.001.
971 Error bars are s.e.m. Scale bars are 500μm for all adult wings images. * p < 0.05,
972 ** p < 0.01, ***p < 0.001 Student's *t*-test.
973
974 **Fig 3. SWI/SNF core components are required for both growth and poste-**
975 **rior fate during wing disc regeneration**
976 (A) Comparison of the size of adult wings after imaginal disc damage and regen-
977 eration in *brm*^{2}/+ and wild-type (*w*^{1118}) animals. n = 142 wings (*brm*^{2}/+) and 224

wings (w^{1118}) from 3 independent experiments, student's t-test $p < 0.001$. (A') Chi-square test $p < 0.001$ across all wing sizes.

(B) Comparison of the size of adult wings after imaginal disc damage and regeneration in animals expressing *Bap111* RNAi and control animals. n = 264 wings (*Bap111* RNAi) and 291 wings (control) from 3 independent experiments. The control for RNAi lines is VDRC 15293 in all experiments, student's t-test $p < 0.01$. (B') Chi-square test $p < 0.001$ across all wing sizes.

(C-G) Adult wing after disc regeneration of wild-type (w^{1118}) (C), $Bap55^{LL05955}$/+ (D), mor^{1}/+ (E), RNAi control (F) or *Bap60* RNAi (G). Anterior is up for all adult wing images. Arrows point to anterior features identified in the posterior compartment. Arrows show five anterior-specific markers in the posterior compartment: anterior crossveins (red), alula-like costa bristles (orange), margin vein (green), socketed bristles (blue), and change of wing shape with wider distal portion of the wing, similar to the anterior compartment (purple).

(H) *moira* expression determined by qPCR of mor^{1}/+, mor^{11}/+ and wild-type (w^{1118}) undamaged wing discs at R24. The graph shows fold change relative to wild-type (w^{1118}) discs.

(I) Comparison of the size of adult wings after imaginal disc damage and regeneration in mor^{11}/+ and wild-type (w^{1118}) animals. n = 114 wings (mor^{11}/+) and 328 wings (w^{1118}) from 3 independent experiments, student's t-test $p < 0.001$. (I') Chi-square test $p < 0.001$ across all wing sizes.

(J) Comparison of the size of adult wings after imaginal disc damage and regeneration in mor^{2}/+ and wild-type (w^{1118}) animals. n = 134 wings (mor^{2}/+) and 414 wings (w^{1118}) from 3 independent experiments, student's t-test $p < 0.05$. (J') Chi-square test $p < 0.001$ across all wing sizes.

(K) Comparison of the size of adult wings after imaginal disc damage and regeneration in animals expressing *brm* RNAi and control animals. n = 234 wings (*brm* RNAi) and 281 wings (control) from 3 independent experiments, student's t-test $p < 0.01$. (K') Chi-square test $p < 0.001$ across all wing sizes.

(L) Adult wing after disc regeneration while expressing *brm* RNAi.

(M) Comparison of the size of adult wings after imaginal disc damage and regeneration in *UAS-osa*/+; *brm* ^{RNAi}/+ and wild-type (w^{1118}) animals. n = 117 wings (*UAS-osa*/+; *brm* ^{RNAi}/+) and 348 wings (w^{1118}) from 3 independent experiments, student's t-test not significant. (M') Chi-square test across all wing sizes $p = 0.058$, not significant at $\alpha = 0.05$ level.

(N) Adult wing after imaginal disc regeneration in *UAS-osa*/+; *brm*^{RNAi}/+ animal.

Error bars are s.e.m. Scale bars are 500μm for all adult wing images. * $p < 0.05$, ** $p < 0.01$, ***$p < 0.001$ Student's *t*-test.

Fig 4. Decreased *Bap170* expression limits regenerative growth and pupariation delay

(A) Wild-type (w^{1118}) regenerating wing disc at R36 with wing pouch marked by anti-Nubbin (green) immunostaining.

(B) *Bap170*$^{\Delta 135}$/+ regenerating wing disc at R36 with wing pouch marked by anti-Nubbin (green) immunostaining.

(C) Comparison of regenerating wing pouch size at 0, 12, 24, and 36 hours after imaginal disc damage in *Bap170*$^{\Delta 135}$/+ and wild-type (w^{1118}) animals.

(D-E) Regenerating wild-type (w^{1118}) (D) and *Bap170*$^{\Delta 135}$/+ (E) wing discs at R24 with Nubbin (green) and PH3 (magenta) immunostaining. Dashed white outline shows the regenerating wing primordium labeled with Nubbin.

(F) Average number of mitotic cells (marked with PH3 immunostaining) in the wing primordium (marked by anti-Nubbin) at R24 in *Bap170*$^{\Delta 135}$/+ and wild-type (*w*^{1118}) animals. n = 8 wing discs (*Bap170*$^{\Delta 135}$/+) and 10 wing discs (*w*^{1118}).

(G-H) Wild-type (*w*^{1118}) (G) and *Bap170*$^{\Delta 135}$/+ (H) regenerating wing discs at R24 with Myc immunostaining.

(I) Quantification of anti-Myc immunostaining fluorescence intensity in the wing pouch in *Bap170*$^{\Delta 135}$/+ and wild-type (*w*^{1118}) regenerating wing discs at R24. n = 9 wing discs (*Bap170*$^{\Delta 135}$/+) and 9 wing discs (*w*^{1118}).

(L) Median time to pupariation for animals during normal development at 18°C. n = 103 pupae (*Bap170*$^{\Delta 135}$/+) and 227 pupae (*w*^{1118}) from 3 independent experiments. Student's *t*-test not significant.

(M) Median time to pupariation for animals after tissue damage (30°C) and regeneration (18°C). n = 117 pupae (*Bap170*$^{\Delta 135}$/+) and 231 pupae (*w*^{1118}) from 3 independent experiments. Because the temperature shift to 30°C in the ablation protocol increases the developmental rate, the pupariation timing of regenerating animals (M) cannot be compared to the undamaged control animals (L). student's t-test $p<0.001$.

(N) *ilp8* expression examined by qPCR of *Bap170*$^{\Delta 135}$/+ and wild-type (*w*^{1118}) regenerating wing discs at R24. The graph shows fold change relative to wild-type (*w*^{1118}) undamaged discs.

(O-Q) Expression of *TRE-Red*, a JNK signaling reporter, in wild-type (*w*^{1118}) undamaged (O), as well as wild-type (*w*^{1118}) (P) and *Bap170*$^{\Delta 135}$/+ (Q) regenerating wing discs at R24. Yellow outline shows the wing disc in (O). White dashed lines show the wing pouch in (P) and (Q) as marked by anti-Nub.

(R) Quantification of *TRE-Red* fluorescence intensity in *Bap170*$^{\Delta 135}$/+ and wild-type (*w*^{1118}) regenerating wing pouches at R24. n = 12 wing discs (*Bap170*$^{\Delta 135}$/+) and 14 wing discs (*w*^{1118}).

(S) *mmp1* expression examined by qPCR of wild-type (*w*^{1118}) and *Bap170*$^{\Delta 135}$/+ regenerating wing discs at R24, and wild-type (*w*^{1118}) undamaged discs. The graph shows fold change relative to wild-type (*w*^{1118}) regenerating discs at R24. Scale bars are 100μm for all wing discs images. * $p < 0.05$, ** $p < 0.01$, *** $p < 0.001$, Student's *t*-test.

Fig 5. Reduction of Osa causes Posterior-to-Anterior transformations during wing disc regeneration

(A) Wild-type (*w*^{1118}) undamaged wing disc with En (green) (A') and Ci (magenta) (A'') immunostaining. DNA (blue) (A''') was detected with Topro3 here and in subsequent panels. Anterior is left for all wing disc images.

(B) Wild-type (*w*^{1118}) regenerating wing disc at R72 with En (green) (B') and Ci (magenta) (B'') immunostaining and DNA (blue) (B''').

(C) *osa*^{308}/+ regenerating wing disc at R72 with En (green) (C') and Ci (magenta) (C'') immunostaining, and DNA (blue) (C'''). Arrowhead points to the low En expression region in which Ci is expressed in the posterior compartment.

(D) Wild-type (*w*^{1118}) undamaged wing disc with Ac immunostaining.

(E) Wild-type (*w*^{1118}) regenerating wing disc at R72 with Ac immunostaining.

(F) *osa*^{308}/+ regenerating wing disc at R72 with Ac immunostaining. Arrowheads show Ac expression in the posterior compartment.

Scale bars are 100μm for all wing discs images.

Fig 6. The BAP complex is required to maintain posterior cell fate during wing disc regeneration

(A) Wild-type (w^{1118}) undamaged wing disc with Ptc (green) (A') and Ci (magenta) (A'') immunostaining.

(B) Wild-type (w^{1118}) regenerating wing disc at R72 with Ptc (green) (B') and Ci (magenta) (B'') immunostaining.

(C) osa^{308}/+ regenerating wing disc at R72 with Ptc (green) (C') and Ci (magenta) (C'') immunostaining. Arrowhead shows Ptc and Ci co-expression in the posterior compartment.

(D) RNAi control regenerating wing disc at R72 with Ptc (green) (D') and Ci (magenta) (D'') immunostaining.

(E) Regenerating wing disc of animals expressing *brm* RNAi at R72 with Ptc (green) (E') and Ci (magenta) (E'') immunostaining. Arrowheads show Ptc and Ci co-expression in the posterior compartment.

Scale bars are 100μm for all wing disc images.

Fig 7. The BAP complex functions in parallel to Tara to prevent P-to-A transformations.

(A-B) Expression of *TRE-Red*, a JNK signaling reporter, in wild-type (w^{1118}) (A) and osa^{308}/+ (B) regenerating wing discs at R24. Dashed white outline shows the regenerating wing primordium as marked by anti-Nub and excluding the debris field.

(C) Quantification of *TRE-Red* expression fluorescence intensity in osa^{308}/+ and wild-type (w^{1118}) regenerating wing pouches at R24. n = 26 wing discs (osa^{308}/+) and 31 wing discs (w^{1118}). Error bars are s.e.m.

(D-F) Tara expression detected with anti- β-gal immunostaining in *tara-lacZ*/+ undamaged (D), *tara-lacZ*/+ R48 (E) and *Bap55*^{LL05955}/+; *tara-lacZ*/+ R48 (F) regenerating wing discs.

(G) Quantification of β-gal expression via fluorescence intensity to determine levels of *tara-lacZ* expression in *Bap55*^{LL05955}/+ and wild-type (*w*^{1118}) regenerating wing pouches at R48. n = 8 wing discs (*Bap55*^{LL05955}/+) and 9 wing discs (*w*^{1118}). Error bars are s.e.m.

(H-J) Adult wings after disc regeneration in wild-type (*w*^{1118}) (H), *osa*^{308}/+ (I) and *UAS-tara*/+; *osa*^{308}/+ (J) animals. Arrows show five anterior-specific markers in the posterior compartment: anterior crossveins (red), alula-like costa bristles (orange), margin vein (green), socketed bristles (blue), and change of wing shape with wider distal portion of the wing, similar to the anterior compartment (purple). Anterior is up for all adult wing images.

(K) Quantification of the number of Posterior-to-Anterior transformation markers described above in each wing after damage and regeneration of the disc, comparing *UAS-tara*/+; *osa*^{308}/+ wings to *osa*^{308}/+ and wild-type (*w*^{1118}) wings, n = 21 wings (*UAS-tara*/+; *osa*^{308}/+), n = 16 wings (*osa*^{308}/+) and n = 34 wings (*w*^{1118}), from 3 independent experiments. *** $p < 0.001$, Chi-square test. Chi-square test measuring *UAS-tara*/+; *osa*^{308}/+ against *w*^{1118}, $p = 0.86$, is not significant.

Scale bars are 100μm for all wing discs images. Scale bars are 500μm for all adult wings images. * $p < 0.05$, ** $p < 0.01$, Student's *t*-test for (C) and (G).

Fig 8. Cell fate changes induce ectopic AP boundaries in the posterior compartment during wing disc regeneration

(A) Wild-type (*w*^{1118}) undamaged wing disc with Ptc (green) (A') and pSMAD (magenta) (A'') immunostaining.

1129 (B) Wild-type (w^{1118}) regenerating wing disc at R48 with Ptc (green) (B') and
1130 pSMAD (magenta) (B'') immunostaining.
1131 (C) osa^{308}/+ regenerating wing disc at R48 with Ptc (green) (C') and Ci (magenta)
1132 (C'') immunostaining.
1133 (D) Proposed working model for the functions of the PBAP and BAP complexes
1134 in regeneration.
1135

Fig 1

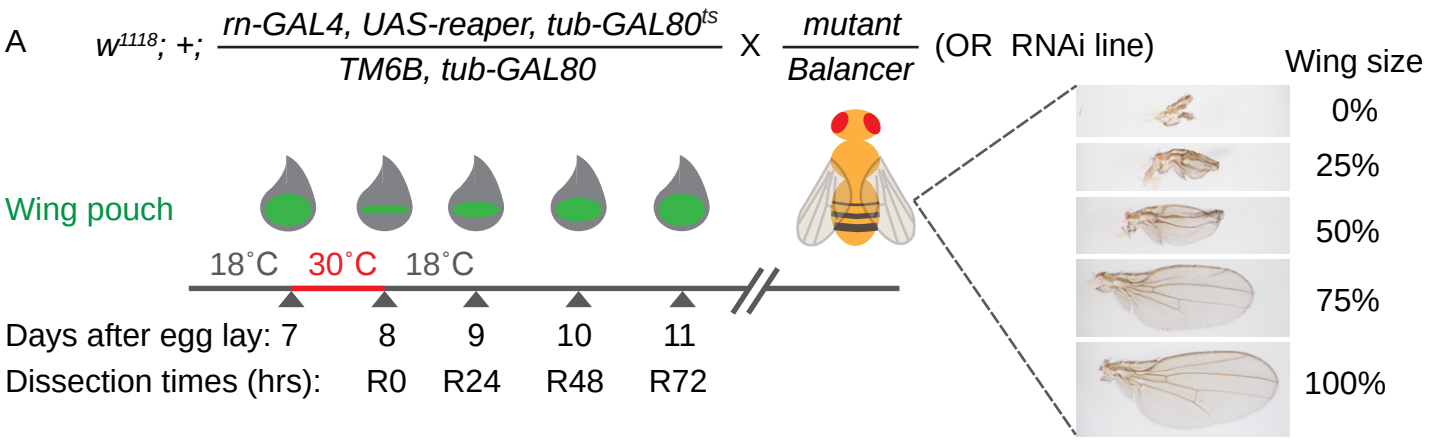

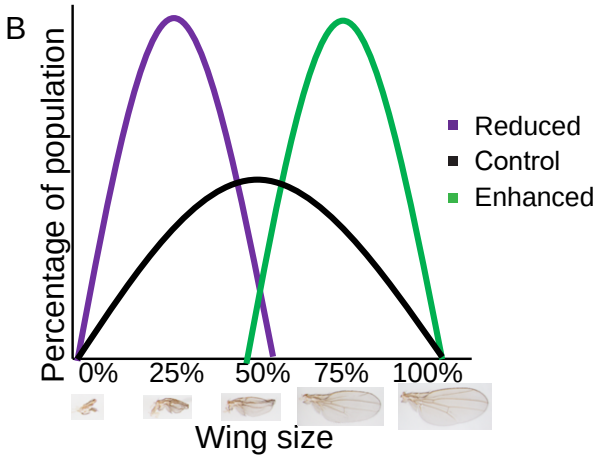

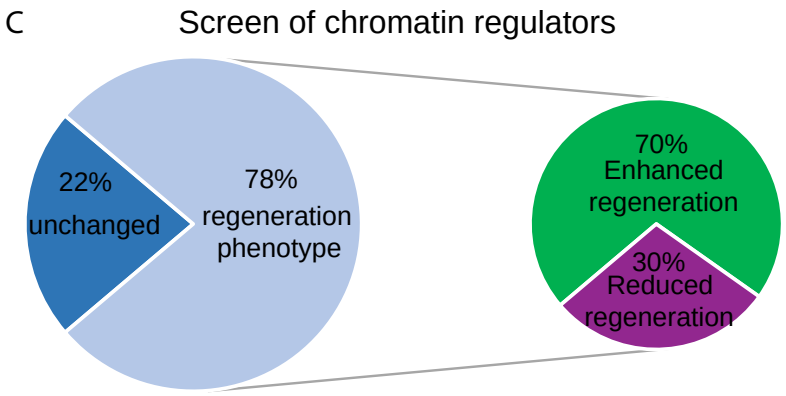

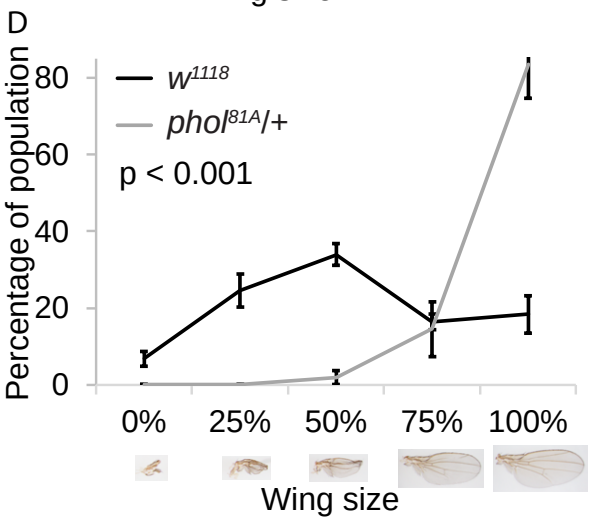

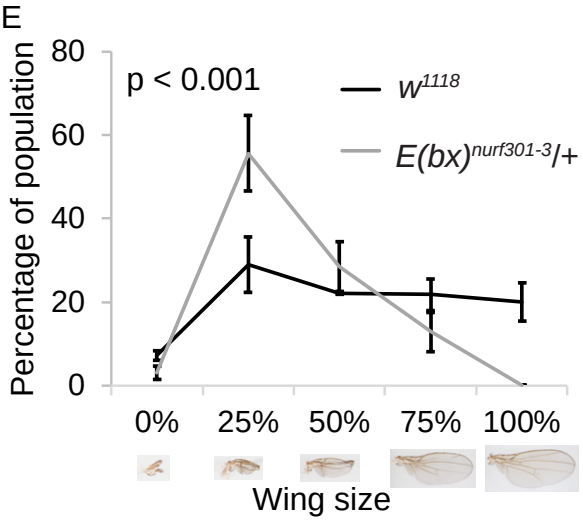

Fig 2

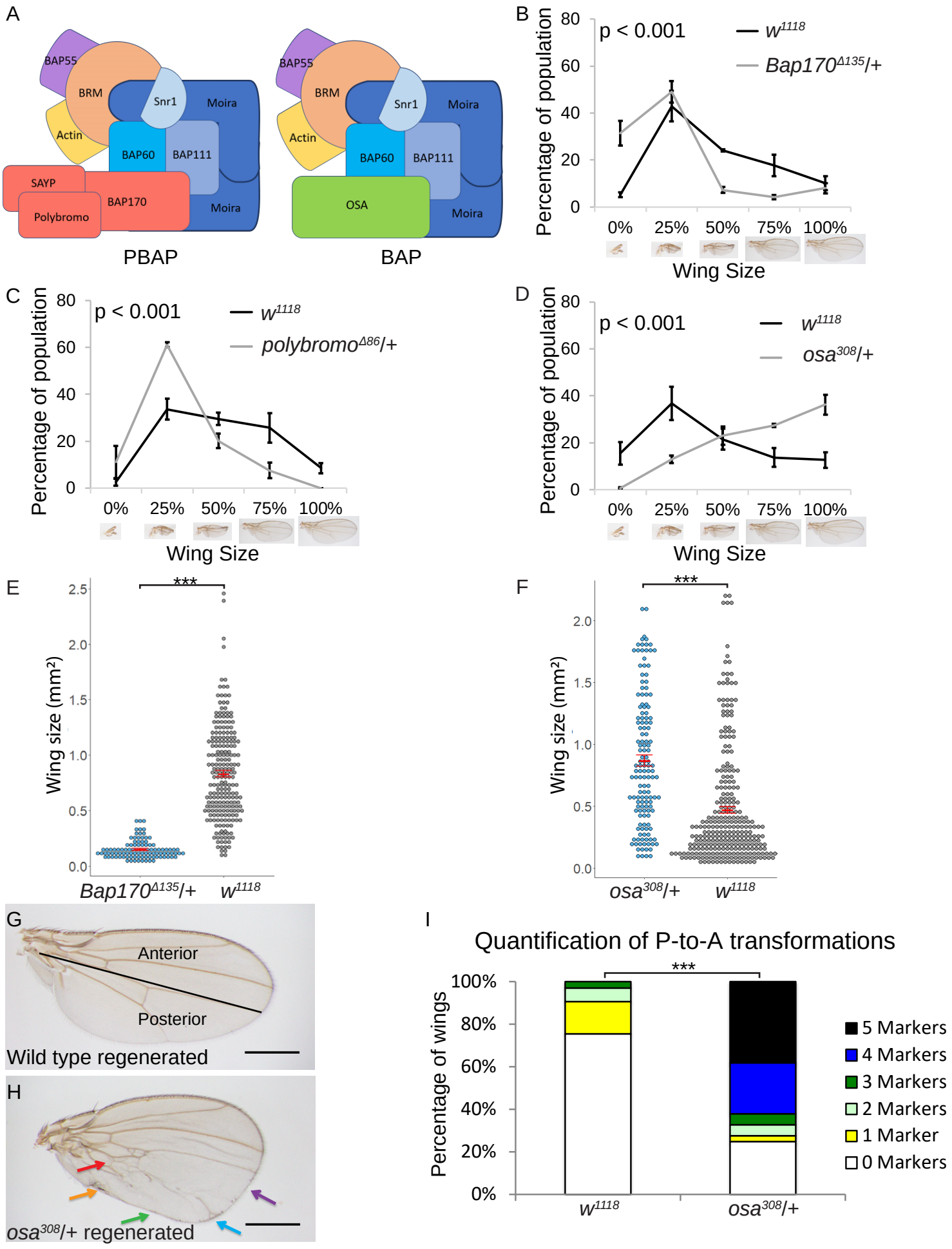

Fig 3

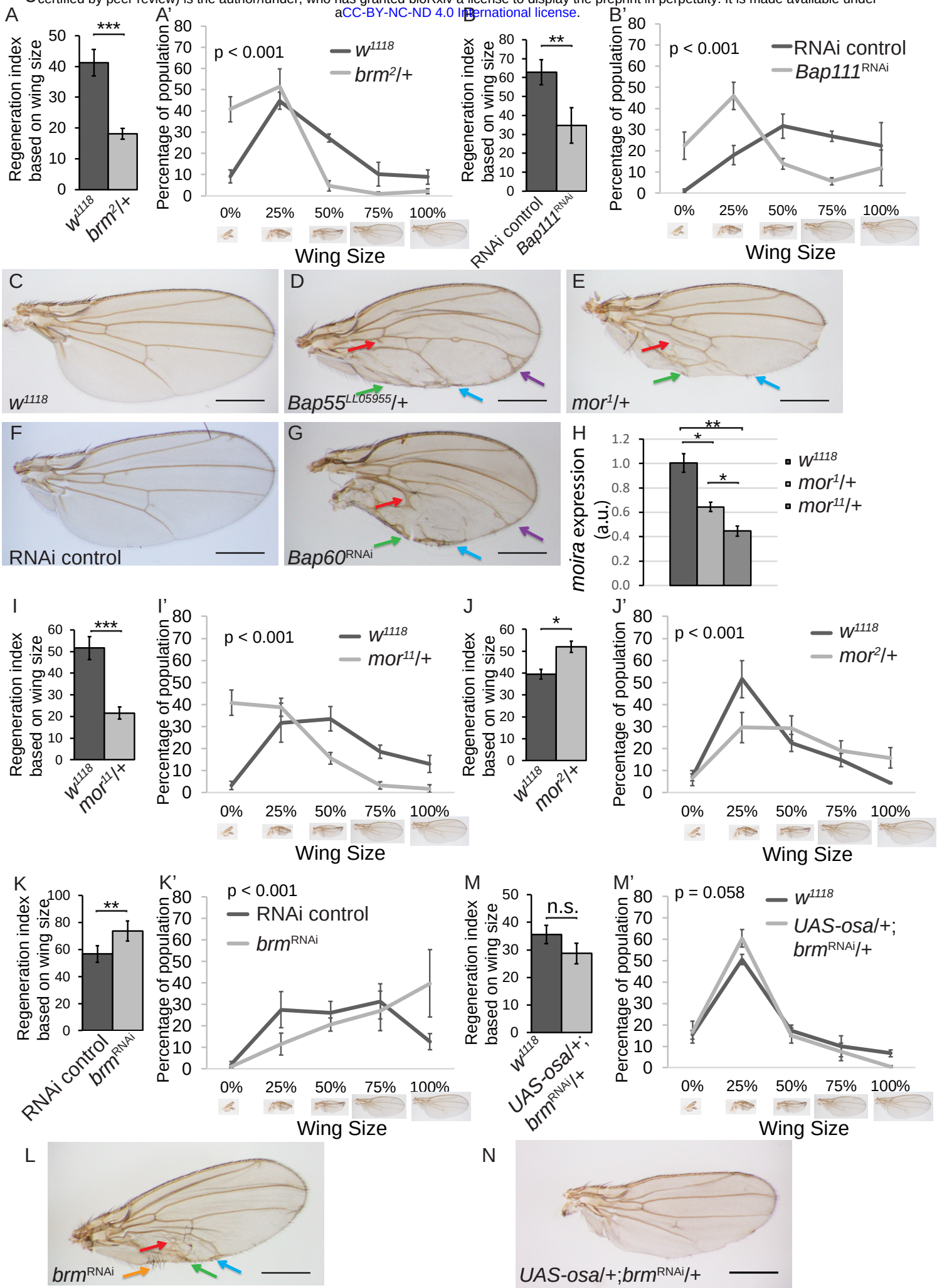

Fig 4

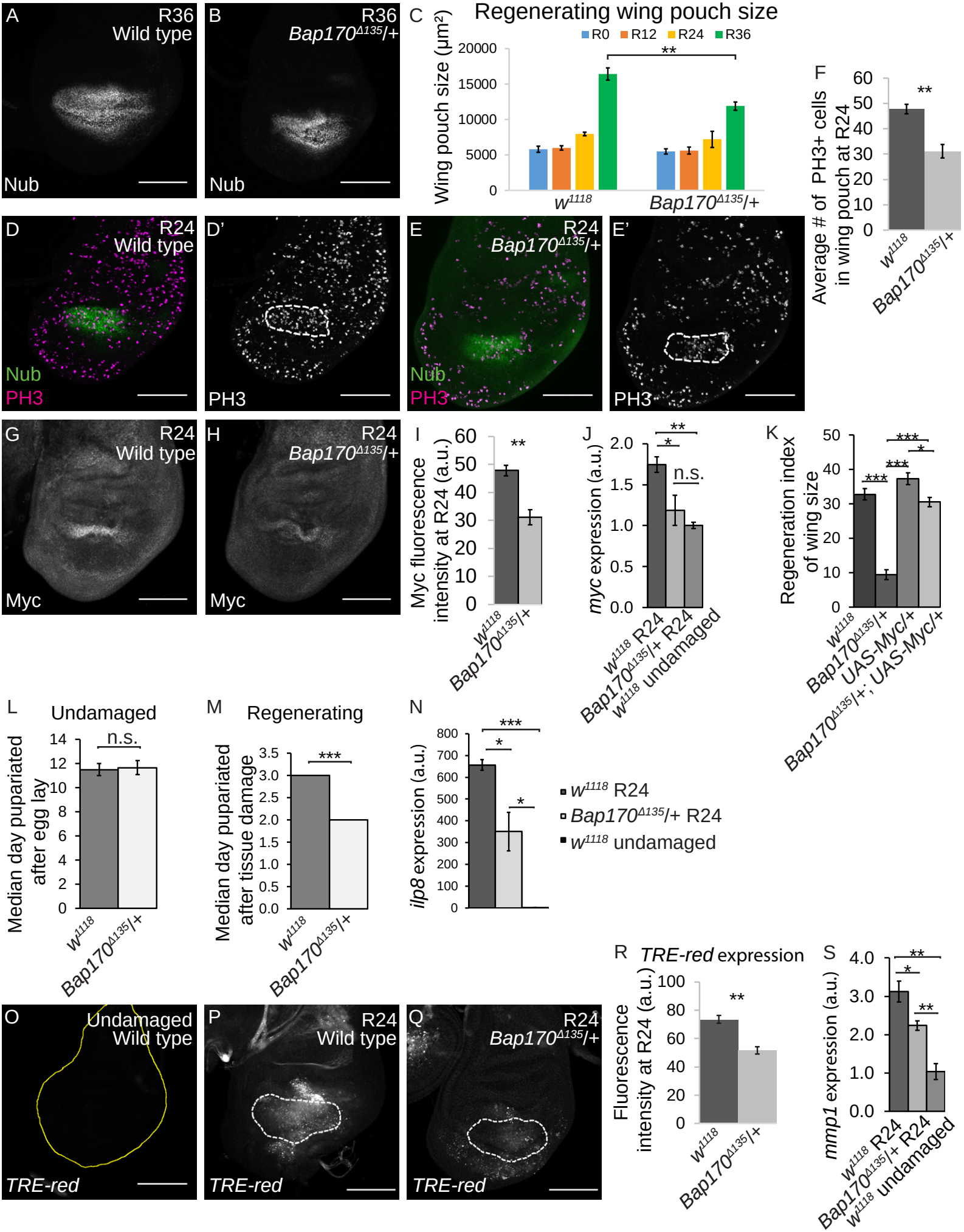

Fig 5

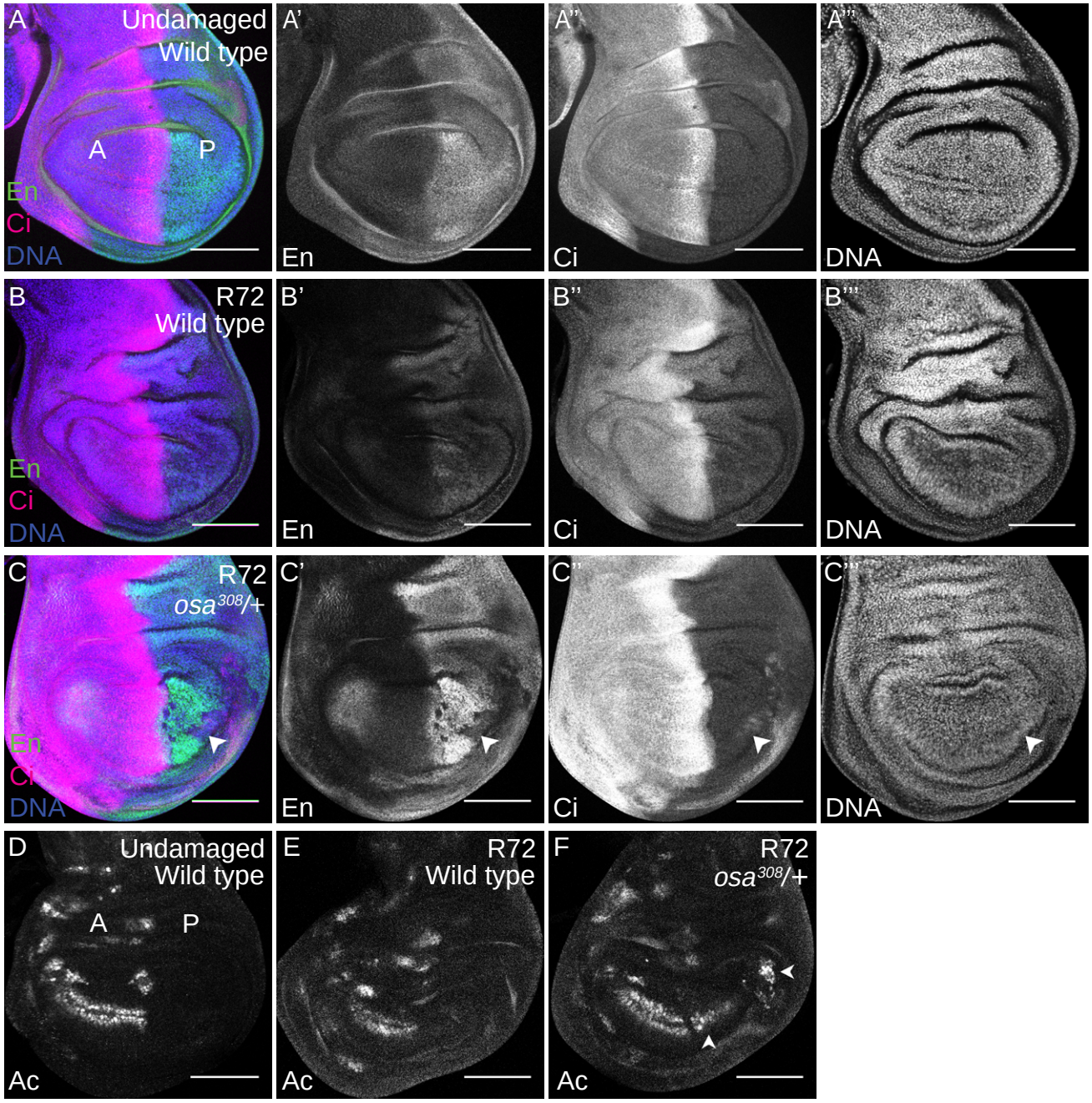

Fig 6

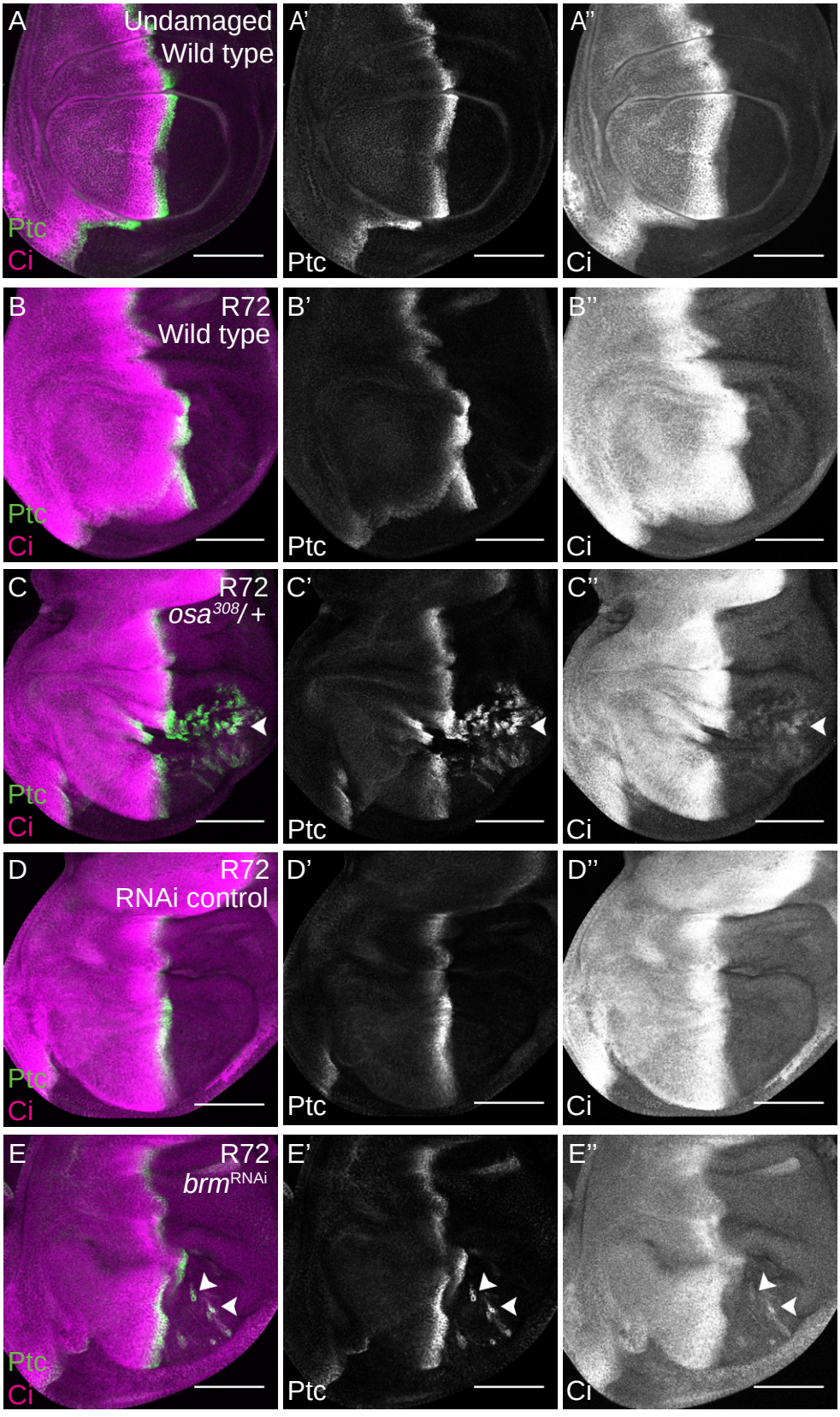

Fig 7

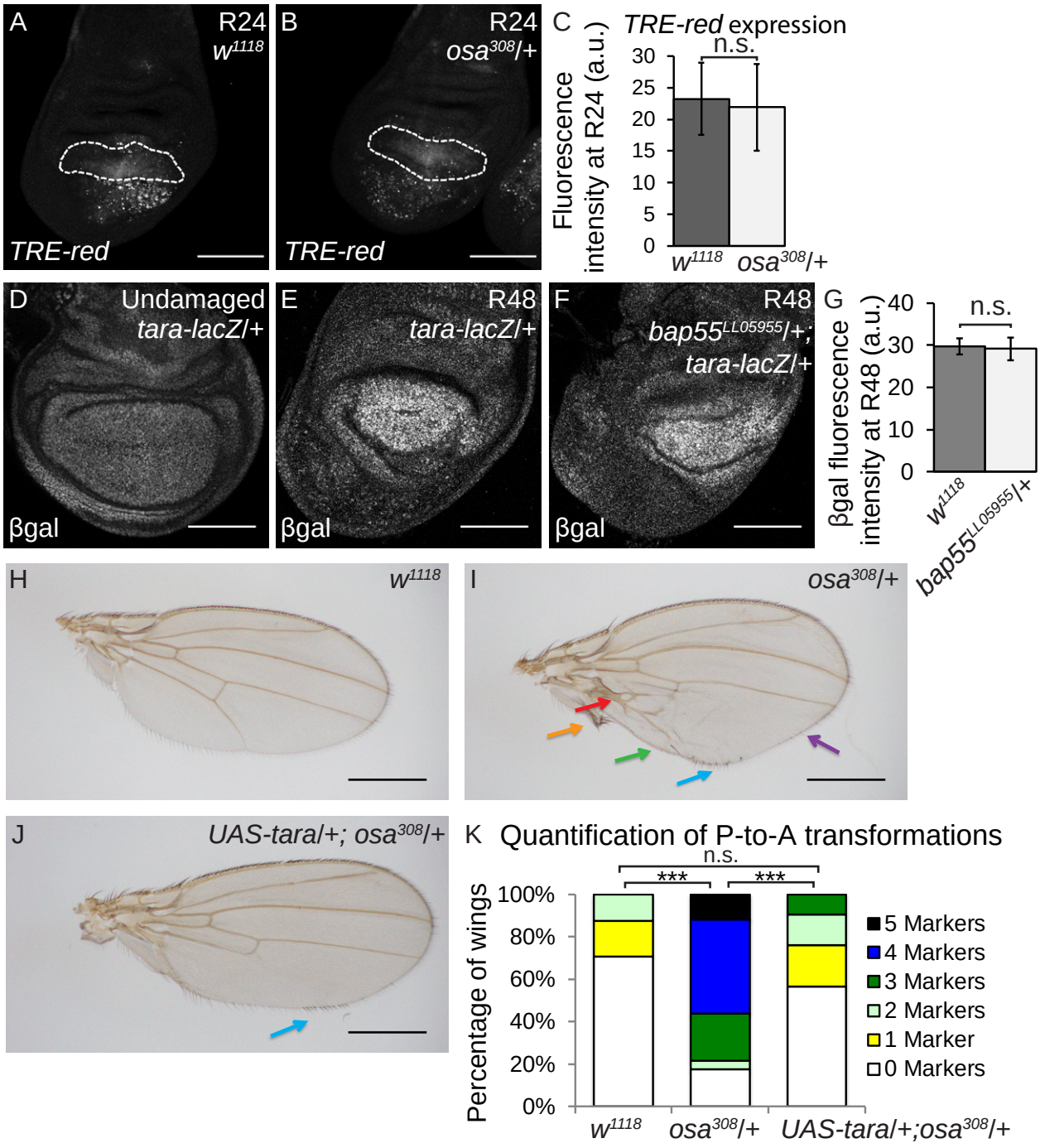

Fig 8